Article

Cell Reports

CD34⁺KLF4⁺ Stromal Stem Cells Contribute to Endometrial Regeneration and Repair

Graphical Abstract

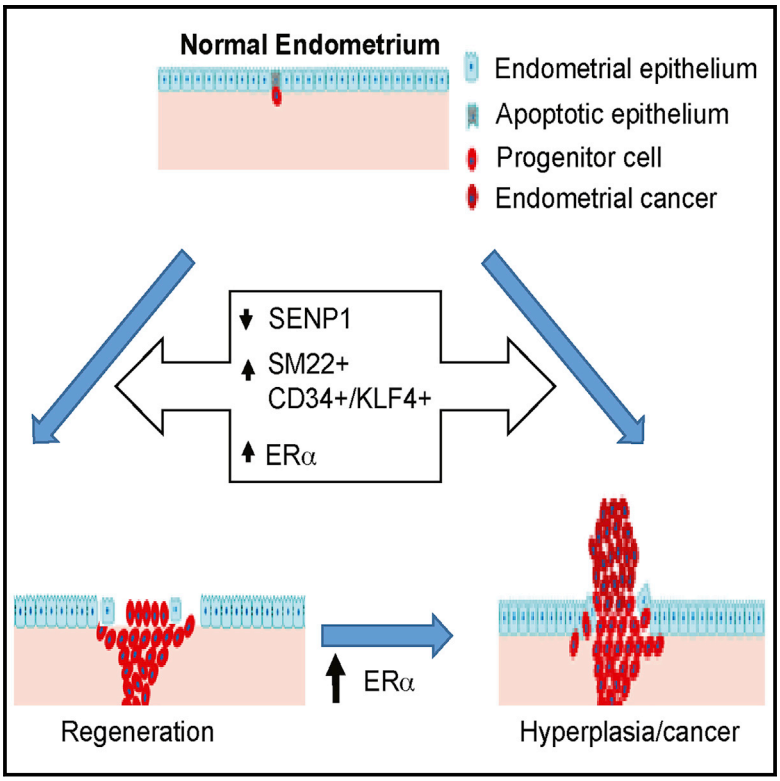

Highlights

- Downregulation or loss of SENP1 induces SUMOylation and activation of ERα
- SENP1-ERα reprograms stromal SM22α⁺ cells into CD34⁺KLF4⁺ progenitor cells
- CD34⁺KLF4⁺ cells migrate to epithelial layer, enhancing endometrial regeneration
- The SENP1-ERα pathway may augment uterine hyperplasia and cancer progression

Authors

Mingzhu Yin, Huanjiao Jenny Zhou, Caixia Lin, ..., Haifeng Zhang, Hugh Taylor, Wang Min

Correspondence

wang.min@yale.edu

In Brief

The regenerative capacity of the human endometrium requires a population of local stem cells. Here, Yin et al. show that uterine stromal SM22α⁺CD34⁺KLF4⁺ stem cells are activated by ERα SUMOylation and integrate into the regeneration area, where they differentiate and incorporate into the endometrial epithelium.

Yin et al., 2019, Cell Reports 27, 2709–2724
May 28, 2019
https://doi.org/10.1016/j.celrep.2019.04.088

CellPress

Cell Reports
Article

CD34$^+$KLF4$^+$ Stromal Stem Cells Contribute to Endometrial Regeneration and Repair

Mingzhu Yin,[1,4] Huanjiao Jenny Zhou,[1] Caixia Lin,[2] Lingli Long,[2] Xiaolei Yang,[2] Haifeng Zhang,[1] Hugh Taylor,[3] and Wang Min[1,5,*]

[1]Interdepartmental Program in Vascular Biology and Therapeutics, Department of Pathology, Yale University School of Medicine, 10 Amistad St., New Haven, CT 06520, USA
[2]Center for Translational Medicine, The First Affiliated Hospital, Sun Yat-sen University, Guangzhou 510080, China
[3]Department of Comparative Medicine and Obstetrics, Gynecology, and Reproductive Sciences, Yale University School of Medicine, New Haven, CT 06510, USA
[4]Present address: Department of Dermatology, Xiangya Hospital, Central South University, and Hunan Key Laboratory of Skin Cancer and Psoriasis, Xiangya Hospital, Central South University, Changsha, Hunan 410008, China
[5]Lead Contact
*Correspondence: wang.min@yale.edu
https://doi.org/10.1016/j.celrep.2019.04.088

SUMMARY

The regenerative capacity of the human endometrium requires a population of local stem cells. However, the phenotypes, locations, and origin of these cells are still unknown. In a mouse menstruation model, uterine stromal SM22α$^+$-derived CD34$^+$KLF4$^+$ stem cells are activated and integrate into the regeneration area, where they differentiate and incorporate into the endometrial epithelium; this process is correlated with enhanced protein SUMOylation in CD34$^+$KLF4$^+$ cells. Mice with a stromal SM22α-specific SENP1 deletion (SENP1smKO) exhibit accelerated endometrial repair in the regeneration model and develop spontaneous uterine hyperplasia. Mechanistic studies suggest that SENP1 deletion induces SUMOylation of ERα, which augments ERα transcriptional activity and proliferative signaling in SM22α$^+$CD34$^+$KLF4$^+$ cells. These cells then transdifferentiate to the endometrial epithelium. Our study reveals that CD34$^+$KLF4$^+$ stromal-resident stem cells directly contribute to endometrial regeneration, which is regulated through SENP1-mediated ERα suppression.

INTRODUCTION

Human endometrial mucosa is a dynamic remodeling tissue, undergoing cyclical morphologic and functional changes in response to fluctuating sex steroid hormones each menstrual cycle in a woman's reproductive life. During these recurring cycles, the endometrial cells lining the uterine cavity proliferate and then are sloughed; however, they are never depleted and do not proliferate out of the normal range (Spencer et al., 2005). If this tight regulation is somehow perturbed, conditions in the uterus adversely influence fertility and can lead to cancer (Bilyk et al., 2017; Gargett, 2004; Gurung et al., 2015). The high regenerative capacity of the human endometrium is absolutely essential for successful reproduction. The process of stromal-to-epithelial transition drives endometrial regeneration at postpartum (after delivery of baby) (Bilyk et al., 2017; Huang et al., 2012; Kalluri and Weinberg, 2009; Pattabiraman and Weinberg, 2014; Patterson et al., 2013). However, the cell population involved in this process and the underlying mechanisms regulating the transition are poorly understood. Endometrial stem cells are also believed to be essential for this regeneration. The first evidence of progenitor stem cells regenerating the endometrium was based on *in vitro* functional assays in which isolated endometrial cells displayed greater self-renewal capability and multipotency (Chan et al., 2004). Further studies suggest that endometrial stem or progenitor cells reside in the basalis layer and persist beyond menopause (Gargett, 2007; Gargett et al., 2014; Schwab et al., 2005; Wolff et al., 2007). Markers specific for endometrial stem cells have yet to be fully characterized. A number of genes associated with endometrial stem cells have been reported, and these genes include stem cell transcriptional factor Oct4, vascular progenitor markers c-Kit (CD117) and CD34, and endometrial carcinoma protein Musashi-1 (Bentz et al., 2010; Cho et al., 2004; Götte et al., 2008; Kato et al., 2007; Kim et al., 2005; Masuda et al., 2010; Matthai et al., 2006; Parasar et al., 2017). CD34 is a transmembrane phosphoglycoprotein, first identified on hematopoietic stem and progenitor cells. Recent data suggest that CD34 is expressed by vascular endothelial progenitors, mesenchymal stem cells (MSCs) and even epithelial progenitor cells (Cho et al., 2004; Kato et al., 2007; Majesky et al., 2017; Sidney et al., 2014). Of note, CD34 along with Sca1 are expressed on vascular adventitia progenitor cells that have the potential to differentiate into multiple lineages. These adventitial Sca1$^+$CD34$^+$ can be generated *in situ* from differentiated smooth muscle cells (SMCs) by upregulating the reprograming transcription factor Kruppel-like factor 4 (KLF4) (Majesky et al., 2017). Similarly, vascular intimal SMCs can gain progenitor phenotypes (Cherepanova et al., 2016; Shankman et al., 2015). It has been proposed that endometrial stem cells are both fetal epithelial and MSCs remaining in the adult endometrium that continue replicating in adulthood, as well as being derived from circulating stem cells arising from a bone marrow niche that seeds the endometrium periodically or in

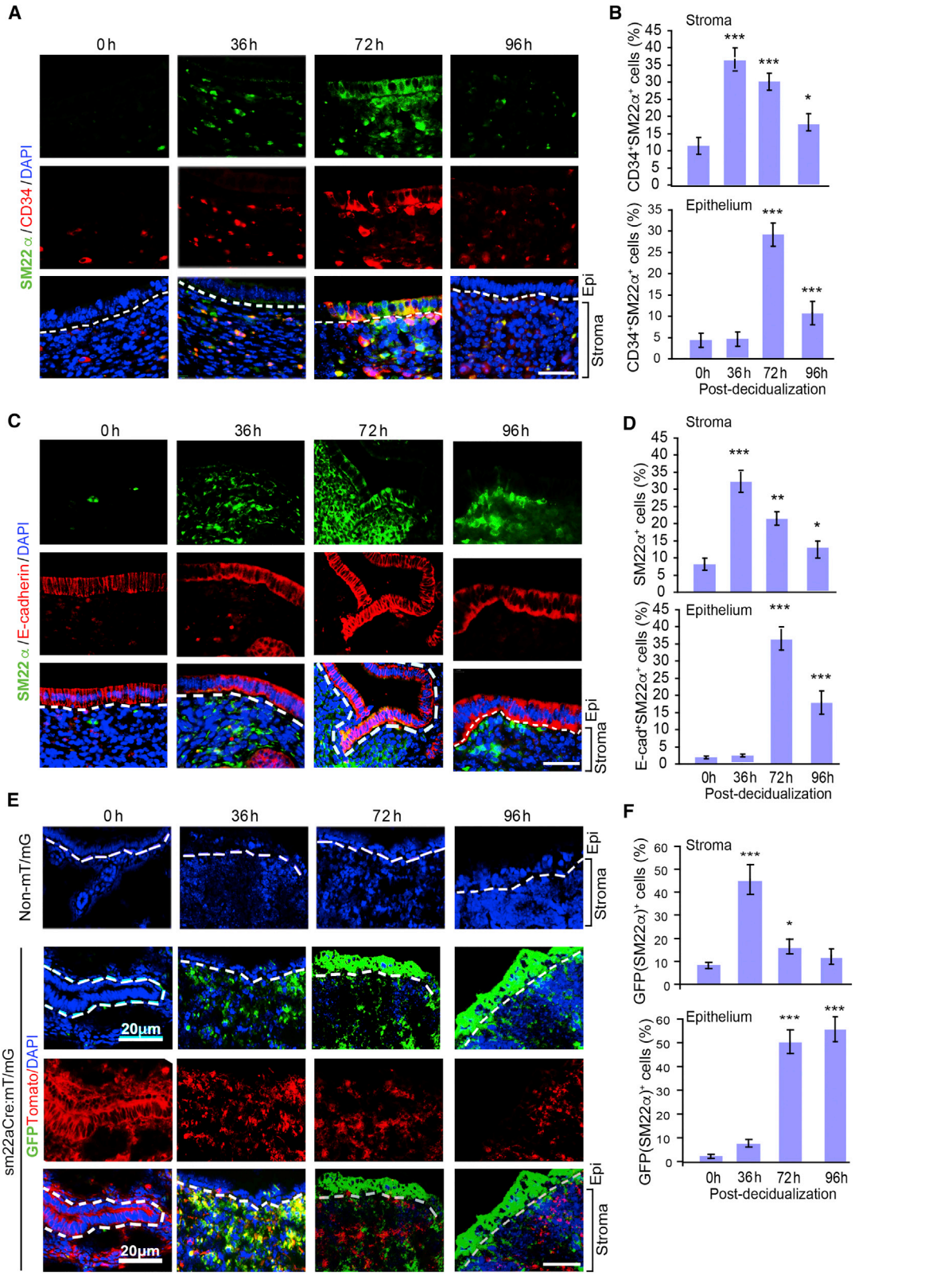

(legend on next page)

response to injury (Du and Taylor, 2007; Figueira et al., 2011; Lynch et al., 2007; Morelli et al., 2012; Taylor, 2004). The strongest evidence supports the presence of a resident MSC population in the uterus (some of which may be derived from bone marrow), but the exact cell types and their regulations have not been well defined.

The small ubiquitin-like modifier (SUMO) can be covalently attached to a large number of proteins through the formation of isopeptide bonds with specific lysine residues of target proteins (Gill, 2004). SUMO molecules include SUMO1, SUMO2, and SUMO3, with SUMO2 and SUMO3 being more abundant (Pickart, 2001; Saitoh and Hinchey, 2000). A consensus SUMO acceptor site has been identified consisting of the sequence ØKXE (Ø is a large hydrophobic amino acid and K is the site of SUMO conjugation). The effect of SUMOylation on protein function is substrate specific, regulating protein stabilization, localization, protein-protein or protein-DNA interactions, and/or biochemical activities. SUMOylation is a dynamic process that is mediated by activating (E1), conjugating (E2), and ligating (E3) enzymes and is readily reversed by a six-member family of SUMO-specific proteases (SUMO endopeptidases [SENPs]) (Müller et al., 2001; Yeh, 2009). SENP1 is ubiquitously expressed, localized in the nucleus and other discrete cellular compartments, and deconjugates a large number of SUMOylated proteins, including nuclear transcriptional factors (Cheng et al., 2007; Yeh, 2009; Yu et al., 2010).

Recently, protein post-translational modification by SUMOylation has been reported to play an important role in embryonic stem cell (ESC) renewal and differentiation (Du et al., 2016; Kota et al., 2017; Sahin et al., 2014; Thiruvalluvan et al., 2018; Wu et al., 2012; Yang et al., 2012). Nanog is a pivotal transcription factor in ESCs and is essential for maintaining the pluripotency and self-renewal of ESCs. SUMOylation of transcription factors Oct4 and Sox2 represses Nanog expression. The function of the SUMO pathway in the endometrium has just begun to be explored (Jiang et al., 2017; Jones et al., 2006; Zheng et al., 2015). Global hypo-SUMOylation and redistribution of SUMO1 conjugates into distinct nuclear foci has been observed to associate with decidualization, a process that results in significant changes to cells of the endometrium in preparation for pregnancy. *In vitro* studies suggest that SUMOylation of the progesterone receptor sensitizes differentiating human endometrial stromal cells to progesterone during decidualization (Jiang et al., 2017; Jones et al., 2006; Zheng et al., 2015). However, little is known about the function and regulation of the SUMO pathway in endometrial stem cells during the menstrual cycle.

In the present study, we have identified a population of SM22α^+-derived CD34$^+$KLF4$^+$ stem or progenitor cells that are located in endometrial stroma, proliferate rapidly after being activated, and migrate to the injured epithelial area, where they participate in endometrial regeneration. Moreover, we show that SENP1 deletion induces SUMOylation of estrogen receptor-α (ERα), which augments ERα transcriptional activity and downstream proliferative signaling in CD34$^+$KLF4$^+$ stem cells, enhancing endometrial regeneration.

RESULTS

SM22α^+CD34$^+$ Stromal-Resident Progenitor Cells Were Involved in Endometrial Regeneration

Cyclical endometrial regeneration occurs in non-menstruating rodents and can be enhanced by exogenous estrogen. We used a mouse menstruation model established by Brasted and colleagues (Brasted et al., 2003; Gurung et al., 2015) and found that epithelial regeneration initiated at 48 h and completed by 96 h post-progesterone withdrawal (Figures S1A and S1B). The expression of several MSC makers (Takahashi and Yamanaka, 2016) was measured, and we found that most of them were increased during endometrial regeneration, especially CD34 and KLF4 (Figure S1C).CD34$^+$ cells were detected among condensed cell populations in the stroma. CD34$^+$ cells were also detected in the regenerative endometrial epithelium, where they were co-stained with E-cadherin, peaking at 72 h but disappearing at the end of repair (96 h) (Figures S1D and S1E).

We reasoned that a group of resident stem or progenitor cells in stroma may participate in endometrial regeneration. We examined several stromal cell markers and found that anti-Mullerian hormone receptor 2 (AMHR2) and the vascular smooth muscle-specific marker SM22α, but not the endothelial cell marker CD31 or lymphatic marker LYVE1, were specifically elevated at 36–96 h post-progesterone withdrawal in repairing the endometrium (Figure S2A). AMHR2 is a well-known stromal marker that is specifically expressed in the mesenchymal cells of the uterus (Arango et al., 2008; Baarends et al., 1994). SM22α is one of the earliest specific markers for differentiated SMCs and perivascular pericytes (Solway et al., 1995). SM22α^+ cells are a subpopulation of AMHR2$^+$ cells in normal stromal cells of the uterus (Figures S2B and S2C). Moreover, SM22α showed co-staining with CD34 in the stroma and in the repairing zone of the endometrium (Figures 1A and 1B, with isotype controls in Figure S2D). Similar to CD34$^+$ cells, SM22α^+ cells were detected only in the stroma at early time points (36 h), but later (72–96 h) were detected in the regenerative

Figure 1. SM22α^+CD34$^+$ Stromal-Resident Progenitor Cells Involved in Endometrial Regeneration

Normal C57BL/6 mice were subjected to induced menstruation, and mouse uteri were harvested at 0, 36, 72, and 96 h post-P4 withdrawal. Tissue sections underwent immunofluorescence staining, and DAPI was used to counterstain cell nuclei.

(A and B) (A) Immunofluorescent staining of SM22α and CD34 in tissue sections, and (B) SM22α^+CD34$^+$ cells in the stroma and epithelium of the mouse uterus were quantified.

(C and D) (C) Immunofluorescent staining of SM22α and E-cadherin in tissue sections, and (D) SM22α^+E-cadherin$^+$ cells in the stroma and epithelium of the mouse uterus were quantified.

(E and F) Normal C57BL/6 mice (non-mT/mG) and sm22αCre:mT/mG mice were subjected to induced menstruation. (E) Representative images and (F) quantification of GFP$^+$ cells in the stroma and endometrium of uterine frozen sections from sm22αCre:mT/mG mice at 0, 36, and 72 h post-P4 withdrawal.

All of the data are presented as means ± SEMs; n = 5; **p < 0.01 and ***p < 0.001 (two-sided Student's t test). Scale bars: 20 μm (A, C, and E).

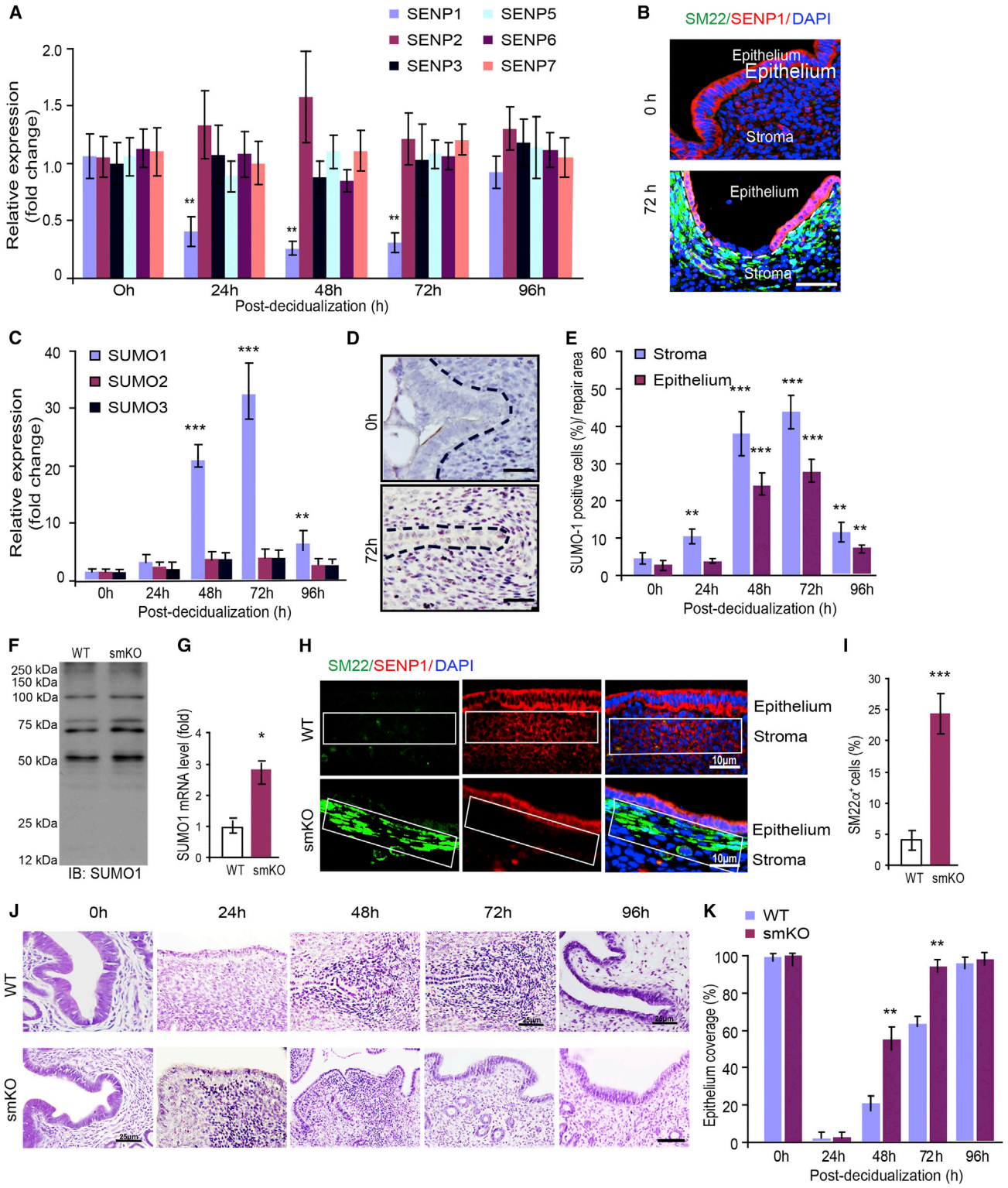

Figure 2. SENP1 Deletion Enhances Epithelium Repair in the Injury Model

Mice were subjected to induced menstruation, and mouse uteri were harvested at 0–96 h post-P4 withdrawal.

(A) SUMOylation and de-SUMOylation family members were determined by qRT-PCR.

(B) SENP1 expression was detected by immunofluorescence staining.

(C) SUMO family members were determined by qRT-PCR.

(legend continued on next page)

endometrial epithelium, where it was co-stained with E-cadherin. However, SM22α$^+$/CD34$^+$ cells almost disappeared by 96 h (Figures 1C and 1D). To further determine whether SM22α stromal cells contribute to endometrium repair, we performed genetic lineage tracing using the *Cre-loxP* system (Kretzschmar and Watt, 2012). Specifically, the SM22α-Cre deleter mice (Lepore et al., 2005) were mated with mT/mG reporter mice to generate sm22α:mT/mG mice so that SM22α$^+$ cells were genetically marked by GFP expression (Lepore et al., 2005; Zong et al., 2005). In addition, SENP1smKO were bred with mT/mG reporter mice to generate Senp1$^{fl/fl}$:sm22α-Cre:mT/mG (called Senp1smKO:mT/G mice). Basal levels of GFP$^+$ (SM22α) cells were few in stroma in SM22α-GFP reporter mice. However, the number of GFP$^+$ (SM22α) cells was drastically increased in the stroma during the early stages of regeneration (36 h) and were subsequently detected in the epithelium at late stages of regeneration (72–96 h) (Figures 1E and 1F). Of note, unlike SM22α$^+$/CD34$^+$ cells, genetically labeled GFP$^+$ cells remained in the regenerative endometrial epithelium at 96 h, even after repair was completed. These data suggest that SM22α$^+$CD34$^+$ progenitor cells, likely derived from stromal resident SM22α$^+$ cells, are directly involved in endometrial regeneration.

Mice with Stromal Deletion of SENP1 Exhibit Accelerated Endometrial Repair and Spontaneous Uterus Hyperplasia with Increased Cell Proliferation and Decreased Cell Death

SUMOylation (SUMO conjugation) and its reverse process de-SUMOylation (SUMO deconjugation) have emerged as important regulatory mechanisms for many biological responses (Müller et al., 2001; Yeh, 2009). However, it has not been shown whether SUMO modification regulates endometrial regeneration. We screened for the expression of different members of the SUMO and de-SUMO systems, and found that only SENP1 expression was greatly reduced during endometrial regeneration (Figure 2A). SENP1 expression was primarily reduced in the stroma by immunofluorescence staining (Figure 2B). SUMO1 (but not SUMO2 and SUMO3) expression was consistently greatly upregulated as detected by qRT-PCR, and the number of SUMO1$^+$ cells was also drastically increased in the uterus. The cells with high SUMO1 expression were localized specifically to the regenerative zones with kinetics similar to the SM22α$^+$CD34$^+$ stromal progenitor cells (Figures 2C–2E). These observations prompted us to investigate the function of SENP1-mediated protein SUMOylation in stromal cells during endometrial regeneration. To this end, we generated mice with an SM22α$^+$ cell-specific deletion of Senp1 by crossing Senp1 floxed-allele mice (Senp1$^{fl/fl}$) with mice in which Cre recombinase expression is driven by the SM22α promoter (Lepore et al., 2005) (called SENP1smKO mice) (Figures S3A–S3C). SENP1 deletion was detected in the endometrial stroma but not in the epithelium of SENP1smKO mice (Figure S3D). SENP1smKO mice were born viable, with normal breeding and body weight before 6 weeks of age. We did not detect significantly increased global levels of SUMO1 conjugation, although SUMO1 expression was increased by ~3-fold in SENP1smKO compared to WT uteri (Figures 2F and 2G). This is possibly due to compensatory regulation of the expression levels or the activity of other SENP and SUMO family members to maintain global levels of SUMO1 conjugation. However, the SENP1 deletion significantly increased SM22α$^+$ cells in the stroma (Figures 2H and 2I). We then compared the kinetics of endometrial regeneration in WT and SENP1smKO mice. Consistent with the role of SM22α$^+$ cells in endometrial repair, the SENP1smKO mice exhibited accelerated endometrial repair in the mouse menstruation model. Specifically, condensed cell population was evident at 24 h post-progesterone withdrawal in SENP1smKO versus 48 h in wild type (WT). Moreover, the epithelium was completely regenerated at 72 h in SENP1smKO compared to WT mice at 96 h post-progesterone withdrawal (Figure 2J, with quantifications in Figure 2K).

We noticed that the number of pups born from pregnant mothers of SENP1smKO mice gradually declined, while the uterus wet weight in the adult female SENP1smKO increased in an age-dependent manner (Figures 3A and 3B). H&E staining showed hyperplasia of endometrial stroma and epithelium in adult SENP1smKO mice compared with age-matched WT mice (Figures 3C and S4A). The incidence of endometrial hyperplasia in SENP1smKO mice varied from 30% at age 1–2 months to 90% at age 12–24 months. Uterine leiomyosarcoma (LMS; a smooth muscle tumor that arises from the muscular part of the uterus) and endometrial cancer were detected in a minority of the old SENP1smKO mice (Figures 3D and S4B). We evaluated cell proliferation and apoptosis in the uteri of SENP1smKO mice by Ki67 and TUNEL staining. Moreover, Ki67 was primarily co-stained with progenitor marker CD34, suggesting that CD34 cells proliferate (Figure S5). The results indicated that the uterine hyperplasia in SENP1smKO mice is due to increased cell proliferation and to decreased cell death in the areas of the endometrial epithelium and stroma (Figures 3E–3H).

SM22α$^+$CD34$^+$ Stromal Progenitor Cells Directly Contribute to Endometrial Hyperplasia

Since we observed a profound increase in SM22α$^+$ cells in SENP1smKO stroma, we determined whether these SM22α$^+$

(D) Immunohistochemical staining of SUMO1 and nuclei were counterstained with hematoxylin.
(E) SUMO1$^+$ cells in the stroma and epithelium were quantified.
(F) Global SUMO conjugation in WT and SENP1smKO uteri were determined by western blotting with anti-SUMO1.
(G) SUMO1 mRNA expression was determined by qRT-PCR.
(H and I) SENP1 deletion in the stroma increased SM22α$^+$ cells. Uteri were harvested at 4–6 weeks of age, and (H) SM22α and SENP1 were stained with respective antibodies followed by DAPI counterstaining.
(I) SM22α$^+$ cells in the stroma (%) were quantified.
(J and K) SENP1 deletion enhances epithelium repair in the injury model. Six-week old WT and SENP1smKO mice were subjected to the mouse endometrial injury model, and uteri were harvested at the indicated times (0–96 h). Representative H&E staining for tissue sections are presented (J), and the percentage of epithelium coverage was quantified (K).
All of the data are presented as means ± SEMs; n = 5; $^{**}p < 0.01$ and $^{***}p < 0.001$ (two-sided Student's t test). Scale bars: 10 μm (B, D, and H) and 25 μm (J).

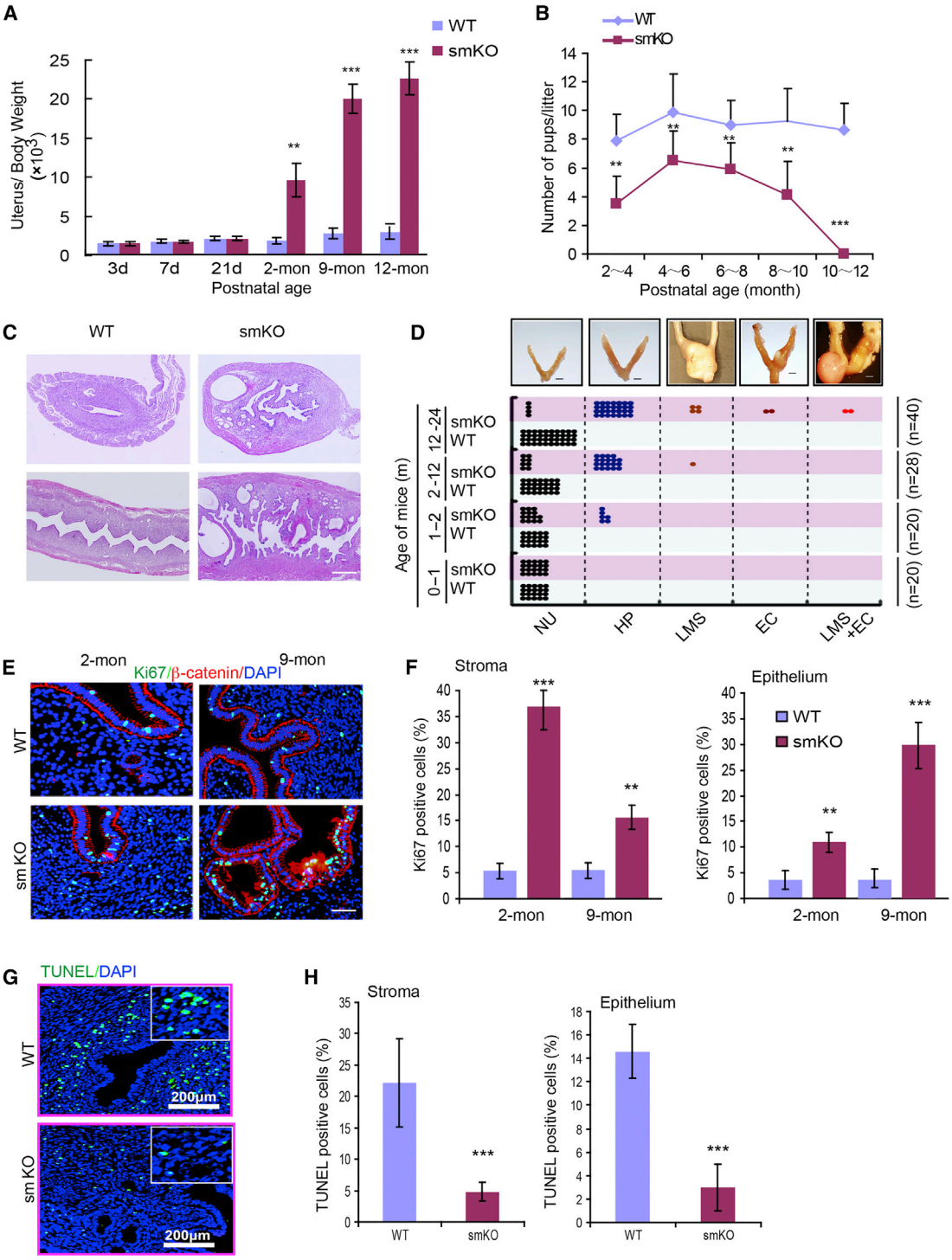

Figure 3. Deletion of SENP1 in Stromal Cells Significantly Induce Uterine Hyperplasia

(A) Quantification of the ratio of uterus over body weight in WT and SENP1smKO mice at different ages.

(B) Quantification of the number of pups in WT and SENP1smKO mice at 2–12 months.

(C) H&E staining of uterus sections from WT and SENP1smKO mice at the age of 9 months. Top: cross-section; bottom: longitudinal section.

(D) Statistical analyses of hyperplasia, uterine sarcoma, and endometrial cancer in WT and SENP1smKO mice observed at different ages.

(E–H) Immunofluorescent staining of Ki67 with epithelial marker β-catenin (E) and TUNEL staining (G) in the uteri of WT and SENP1smKO mice at the age of 2 and 9 months. Proliferating ($Ki67^+$) and apoptotic ($TUNEL^+$) cells were quantified in (F) and (H).

All of the data are presented as means ± SEMs; n = 5; $^{**}p < 0.01$ and $^{***}p < 0.001$ (two-sided Student's t test). Scale bars: 600 μm (C) and 200 μm (E and G).

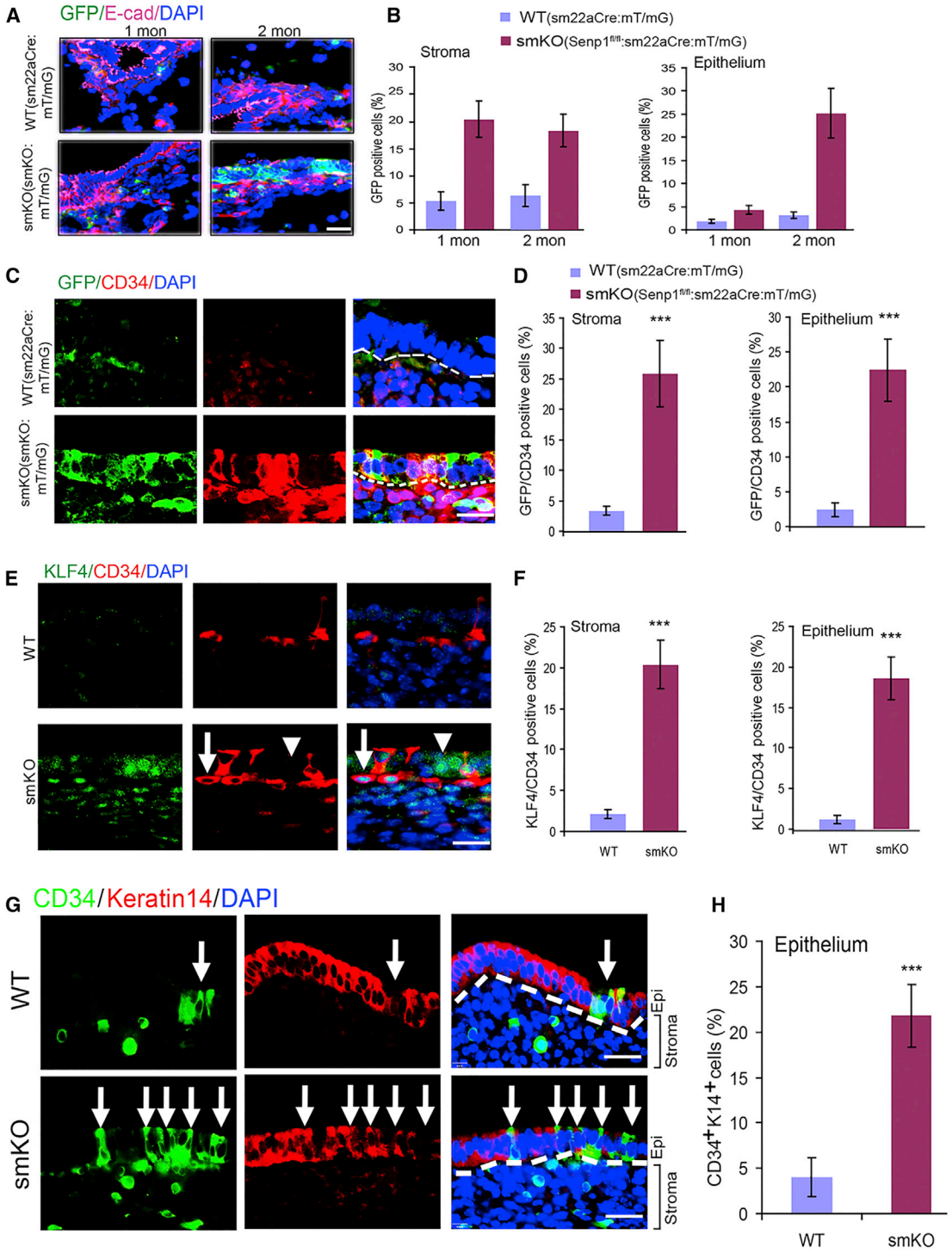

Figure 4. SM22α$^+$CD34$^+$ Stromal Progenitor Cells Directly Contribute to Uterine Hyperplasia

(A) Immunofluorescent staining with allophycocyanin (APC)-conjugated anti-E-cadherin shown in purple in uterine sections from mT/mG reporter mice (WT) and SENP1smKO:mT/mG mice at the age of 1 and 2 months. DAPI was used for counterstaining of cell nuclei.

(B) GFP$^+$ as indicative SM22α$^+$ cells in the stroma and epithelium layer was quantified.

(C and D) Immunofluorescent staining (C) and quantification (D) of CD34 and co-localization with GFP (SM22α) in uterine sections of 2-month-old WT and SENP1smKO mice.

(legend continued on next page)

incorporate into the epithelium and contribute to uterine hyperplasia. To this end, we established mT/mG:SM22αCre and SENP1smKO:mT/mG (Senp1$^{fl/fl}$:mT/mG:SM22αCre) mouse lines and traced GFP$^+$ cells during endometrium regeneration. We observed greater numbers of GFP$^+$ cells in endometrial stroma at 1 month of age and in the epithelium after 2 months of age in the SENP1smKO:mT/mG mice, in which GFP$^+$ cells showed co-staining with epithelial cell marker E-cadherin (Figures 4A, 4B, and S6A). Moreover, a strong co-localization of GFP with CD34 and SM22α in the SENP1smKO:mT/mG uterus was detected. The number of GFP$^+$/CD34$^+$ and SM22α$^+$/CD34$^+$ cells was significantly increased in endometrial stroma and epithelium in SENP1smKO:mT/mG mice (Figures 4C and 4D). We also found the marker of MSCs, KLF4 (Cherepanova et al., 2016; Majesky et al., 2017; Shankman et al., 2015; Wen et al., 2016), had increased and was co-localized with CD34$^+$ cells (Figures 4E and 4F). Of note, KLF4 nuclear staining was evident in CD34$^+$ cells, while KLF4 cytoplasmic staining was detected in CD34$^-$ cells in the epithelium layer, where they may undergo mesenchymal-to-epithelial cell transition (MET). Furthermore, co-staining with E-cadherin and keratin 14 further confirmed the localization of CD34$^+$ cells to the epithelium, where again we observed greater numbers of CD34$^+$/E-cadherin$^+$ or CD34$^+$/keratin 14$^+$ cells in SENP1smKO mice (Figures 4G, 4H, S6B, and S6C). Although controversial, recent work has suggested that bone marrow-derived cells that reach the uterus are CD45$^+$ leukocytes, but they do not contribute to endometrial cell lineage in chimeric mouse models (Ong et al., 2018). We have performed CD45 staining and confirmed that there were few intraepithelial leukocytes at the basal level. Although CD45$^+$ cells were significantly increased within stroma in the injury and repair model, no differences were detected between WT and SENP1smKO mice. Moreover, CD45$^+$ cells were detected in the epithelium layer (Figures S6D–S6F). Our data have shown that SM22α$^+$CD34$^+$KLF4$^+$ stem cell or progenitor cells in uterine stroma directly contribute to endometrial hyperplasia and regeneration, which is greatly augmented by the SENP1 deletion.

To further confirm the SM22$^+$/CD34$^+$KLF4$^+$ triple positive cells, GFP$^+$CD34$^+$ cells were collected by fluorescence-activated cell sorting (FACS) from the uteri of WT:mT/mG and SENP1smKO:mT/mG mice followed by the detection of KLF4 expression and KLF4$^+$ cells. GFP$^+$CD34$^+$ cells were highly abundant in SENP1smKO mice compared to WT mice, and these GFP$^+$CD34$^+$ cells (but not GFP$^+$CD34$^-$ cells) expressed KLF4 (Figures 5A–5D). To directly test whether SM22$^+$/CD34$^+$ cells could differentiate into epithelial cells, SM22$^+$/CD34$^+$ cells were cultured in the absence or presence of 17-β estradiol (E2; 10 nM) for 10 days. Approximately 40% of SM22α$^+$/CD34$^+$ cells displayed the morphological changes after E2 treatment. We found that both GFP$^+$/CD34$^-$ and GFP$^+$/CD34$^+$ cells express the mesenchymal marker vimentin, with no epithelial cell marker E-cadherin. However, treatment with E2 induced MET, in which cells lost vimentin with a concomitant gain of E-cadherin expression (Figures 5E and 5F). To functionally confirm that the subset of epithelial-like SM22α$^+$/CD34$^+$ cells were epithelial cells, we established a 3D Matrigel endometrial formation model (Arnold et al., 2001, 2002). Results showed that GFP$^+$CD34$^+$ cells could form typical endometrium structures, a process that was further enhanced in the presence of E2 (Figures 5G and 5H). These data suggest that SM22α$^+$CD34$^+$ stromal mesenchymal cells undergo transdifferentiation, contributing to endometrial hyperplasia.

ERα SUMOylation Augments ERα Transcriptional Activity

Estrogen and ERα is a major hormone ligand and receptor involved in the menstrual cycle (Edery et al., 1989; Yamashita et al., 1989). The observation that SM22α$^+$CD34$^+$ stromal mesenchymal cells undergo estrogen-dependent transdifferentiation prompted us to test whether SENP1/SUMOylation could modulate ER transcriptional activity (Hilmi et al., 2012; Wen et al., 2016). To this end, we measured 17-β estradiol levels in blood samples by ELISA, and no difference was detected between WT and SENP1smKO mice (Figure S7A). We then measured the gene expression of ERα in uteri from different ages of WT and SENP1smKO mice and found that the expression of ERα was significantly increased in adult SENP1smKO mice as detected by qRT-PCR and western blot (Figures S7B–S7D). Immunochemistry staining indicated that the number of ERα$^+$ cells was increased in both stroma and epithelium (Figures 6A and 6B). The downstream target of ERα, cyclin D1, is known as a strong regulator of cell proliferation (Wang et al., 2015; Zwijsen et al., 1997). Immunostaining assays and western blot revealed an increase in cyclin D1 expression in the SENP1smKO uterus (Figures 6C, 6D, and S7E–S7G).

We next considered whether SUMOylation may enhance ERα activity and ERα-mediated proliferation in stromal progenitor cells. An extra band above ERα protein was observed in the SENP1smKO uterus, suggesting an increase in ERα SUMOylation. Endogenous ERα underwent SUMOylation by SUMO1 in SM22α$^+$ cells as detected by a co-immunoprecipitation assay, and the ERα SUMOylation level was significantly higher in SENP1smKO mice (Figures 6E–6G). ERα SUMOylation was further confirmed in an overexpression system in which ERα (with FLAG tag) and SUMO1 (with hemagglutinin [HA] tag) were co-expressed in human stromal cells followed by co-immunoprecipitation assays (Figure 6H). Multiple lysine residues on ERα have been previously identified as potential SUMOylation sites (Hilmi et al., 2012). However, our mutagenesis assays

(E and F) Co-immunofluorescent staining (E) and quantification (F) of KLF4 and CD34 in uterine sections of 2-month-old WT and SENP1smKO mice. Arrow indicates a typical nuclear KLF4-staining CD34$^+$ progenitor cell, while the arrowhead indicates CD34$^-$ cells located in the epithelium layer with KLF4-cytoplasmic staining.

(G and H) Co-immunofluorescent staining (G) and quantification (H) of CD43 and epithelial marker keratin 14 in uterine sections of 2-month-old WT and SENP1smKO mice. White dashed lines show the boundaries between the endometrial stroma and epithelium. White arrows show CD34$^+$ keratin 14$^-$ cells in the epithelial layer.

All of the data are presented as means ± SEMs; n = 5; $^{**}p < 0.01$ and $^{***}p < 0.001$ (two-sided Student's t test). Scale bars: 20 μm (A, C, E, and G).

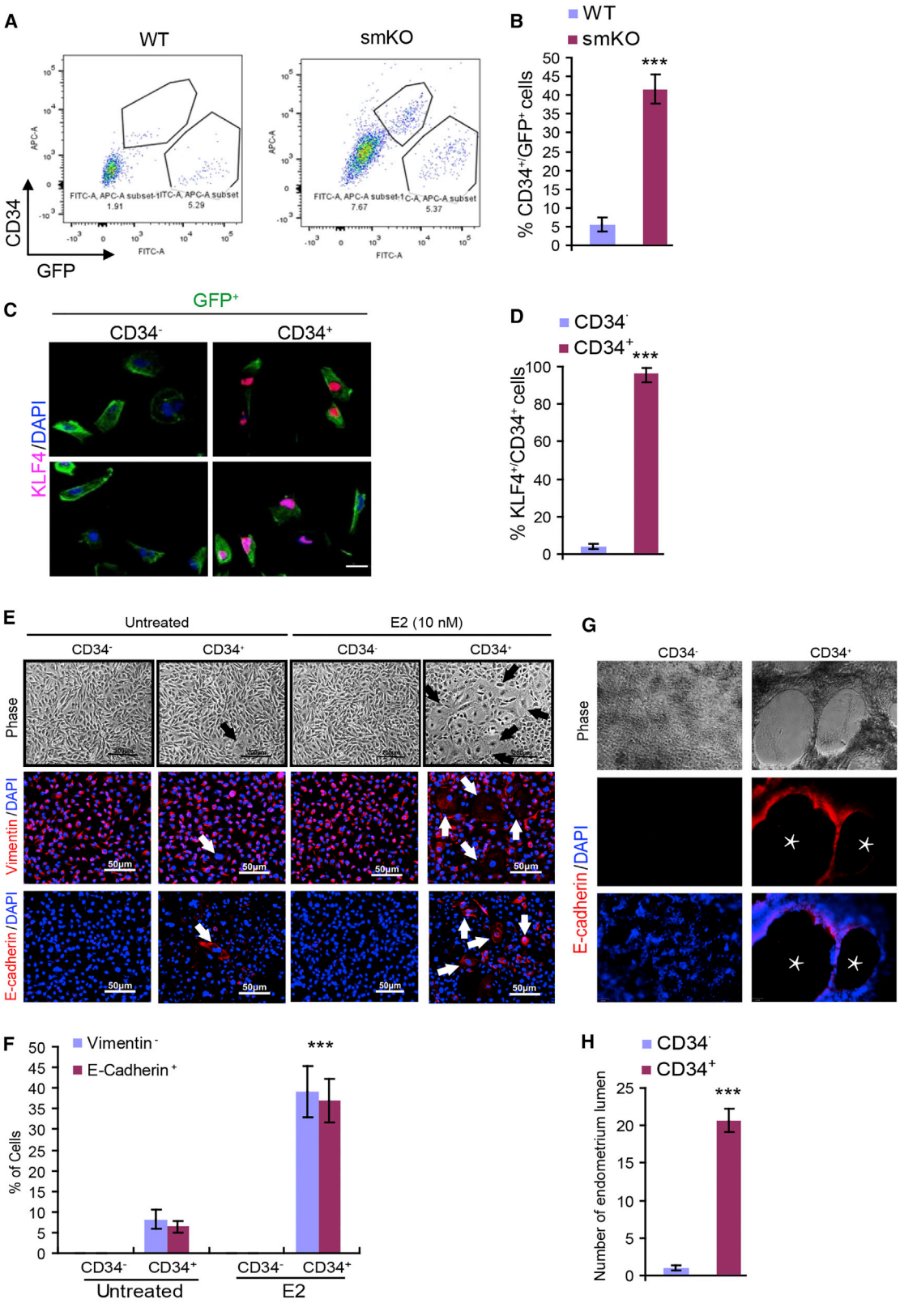

(legend on next page)

indicated that mutation at just a single putative SUMOylation lysine-472, but not three other sites (lysine-171, -180, or -299), diminished the ERα SUMOylation in SENP1-deficient cells (Figure 6I), suggesting that K472 is a critical SUMOylation site for ERα induced by the SENP1 deletion. By reconstitution of ERα mutants into human stromal cells, we found that K472 mutation significantly reduced its transcriptional activity on the gene expressions of cyclin D1 and insulin growth factor 1 (IGF1), which are positive regulators in uterine cell proliferation (Suzuki et al., 2007) (Figure 6J). These results demonstrated that SENP1 deletion not only increases ERα expression but also augments ERα SUMOylation and SUMOylation-mediated gene expression of ERα downstream proliferative signaling (Heldring et al., 2007; Nephew et al., 2000). A previous report suggested that SUMOylation of ERα at several sites (including K472) by SUMO3 was associated with transcriptional suppression of estrogen responses by the antiestrogen fulvestrant in cell lines. The different effects of SUMOylation on ERα transcriptional activity is possibly due to distinct SUMO molecules conjugated (SUMO1 versus SUMO3) and/or conjugation at one versus multiple sites.

ERα SUMOylation Augments Stem Cell Proliferation and Endometrial Hyperplasia

To investigate our observation that ERα SUMOylation and expression has clinical relevance, we examined the expression of SUMO1 and ERα by immunohistochemistry (IHC) in clinical endometrial samples with normal, atypical hyperplasia or cancer histological features. SUMO1 expression was low in normal endometrium and weakly upregulated in atypical hyperplasia, but it was drastically increased in endometrial cancer samples. A similar pattern was observed for ERα expression. Moreover, there was a clear correlation between SUMO1 with ERα scores and $CD34^+$ cells in clinical samples (Figures S8 and S9).

To investigate the role of increased ERα expression and activity in the uterine hyperplasia observed in SENP1smKO mice, we examined whether ERα was expressed in endometrial stem cells. Immunofluorescent staining showed that ERα is specifically upregulated in $CD34^+$ cells. Moreover, $ER\alpha^{high}CD34^+$ cells are highly increased in both endometrial stroma and epithelium in SENP1smKO mice (Figures 7A and 7B). To prove that ERα is an important pathway for regulating uterine hyperplasia in the SENP1smKO mice, we used a genetic rescue approach by crossing SENP1smKO with $ER\alpha^{+/-}$ mice. $ER\alpha^{-/-}$ homozygous female mice were sterile, whereas $ER\alpha^{+/-}$ female mice had a normal uterine size and function (Dupont et al., 2000). The deletion of a single allele of ERα in SENP1smKO (smKO/$ER\alpha^{+/-}$) female mice diminished uterine hyperplasia compared to SENP1smKO (Figures 7C and 7D) with a normalized number of endometrial $CD34^+KLF4^+$ progenitor cells (Figures 7E and 7F). These data suggest that augmented ERα is critical for stromal $SM22^+$-derived $CD34^+KLF4^+$ progenitor cell proliferation and endometrial hyperplasia in SENP1smKO mice.

DISCUSSION

The most significant finding from our study is that we have identified that stromal SM22α-derived $CD34^+KLF4^+$ cells function as endometrial stem cells in several different mouse models. By immunofluorescence staining and lineage tracing with a GFP labeling approach, we show that the $SM22\alpha^+$ stromal cells are activated in response to an estrogen stimulation, gaining marker expression of $CD34^+KLF4^+$ progenitor cells. By examining the localization of $CD34^+KLF4^+$ cells at various time points during endometrial repair, we have shown that $SM22\alpha^+CD34^+KLF4^+$ cells are present in the stroma at an early phase, but are localized in the regenerating epithelial layer during repair. Those integrated $CD34^+KLF4^+$ cells gradually lose stem cell markers CD34 and KLF4 but gain the epithelial markers E-cadherin and keratin 14. Furthermore, an *in vitro* 3D Matrigel model shows that $SM22\alpha^+CD34^+$ stromal mesenchymal cells undergo mesenchymal-to-epithelial transition (MET). These data indicate that stromal $SM22\alpha^+CD34^+$ cells likely migrate to the regeneration area, where they incorporate into the endometrial epithelium. We further show that ERα and its downstream proliferative signaling in $CD34^+KLF4^+$ cells are highly activated during regeneration; ERα signaling is activated by the deletion of SENP1, leading to a substantial increase in the number of $SM22\alpha^+CD34^+KLF4^+$ cells and to endometrial regeneration in SM22α-specific SENP1-deficient mice. Our study supports that SM22α-derived $CD34^+KLF4^+$ stromal-resident stem cells directly contribute to endometrial regeneration. The exact mechanism by which $CD34^+KLF4^+$ cells undergo MET is unclear. Our observation that co-expression of KLF4 with active ERα in migrating cells suggests that the reprogramming factor KLF4 may play a very important role in the MET process. Therefore, we propose the following model: ERα activation activates KLF4, which reprograms stromal $SM22\alpha^+$ cells into $CD34^+KLF4^+$

Figure 5. $SM22\alpha^+CD34^+$ Stromal Mesenchymal Cells Transdifferentiate into Epithelial Cells *In Vitro*

(A–D) $SM22\alpha^+CD34^+$ stromal mesenchymal cells express KLF4.

(A) FACS analyses and sorting of GFP^+CD34^+ stromal mesenchymal cells from the uteri of 2-month-old mT/mG reporter mice (WT) and SENP1smKO:mT/mG mice.

(B) The percentage of $CD34^+/GFP^+$ cells was quantified.

(C and D) (C) GFP^+CD34^+ and GFP^+CD34^- cells were subjected to immunofluorescence staining with KLF4, and (D) the percentage of $KLF4^+/CD34^+$ cells were quantified.

(E and F) $SM22\alpha^+CD34^+$ stromal mesenchymal cells transdifferentiation to epithelial cells. Sorted GFP^+CD34^+ and GFP^+CD34^- cells were cultured in the absence or presence of E2 (10 ng/mL) for 10 days. (E) Cells were subjected to immunostaining for vimentin and E-cadherin, and (F) the percentage of positive cells was quantified.

(G and H) Endometrium formation analyses. GFP^+CD34^+ and GFP^+CD34^- cells were cultured in a Matrigel-precoated 24-well plate.

(G) The cells were incubated 6–48 h to allow the formation of endometrial-like structures with lumens.

(H) The number of endometrium formations was quantified based on phase and fluorescence images.

All of the data are presented as means ± SEMs; n = 6; $^{**}p < 0.01$ and $^{***}p < 0.001$ (two-sided Student's t test).

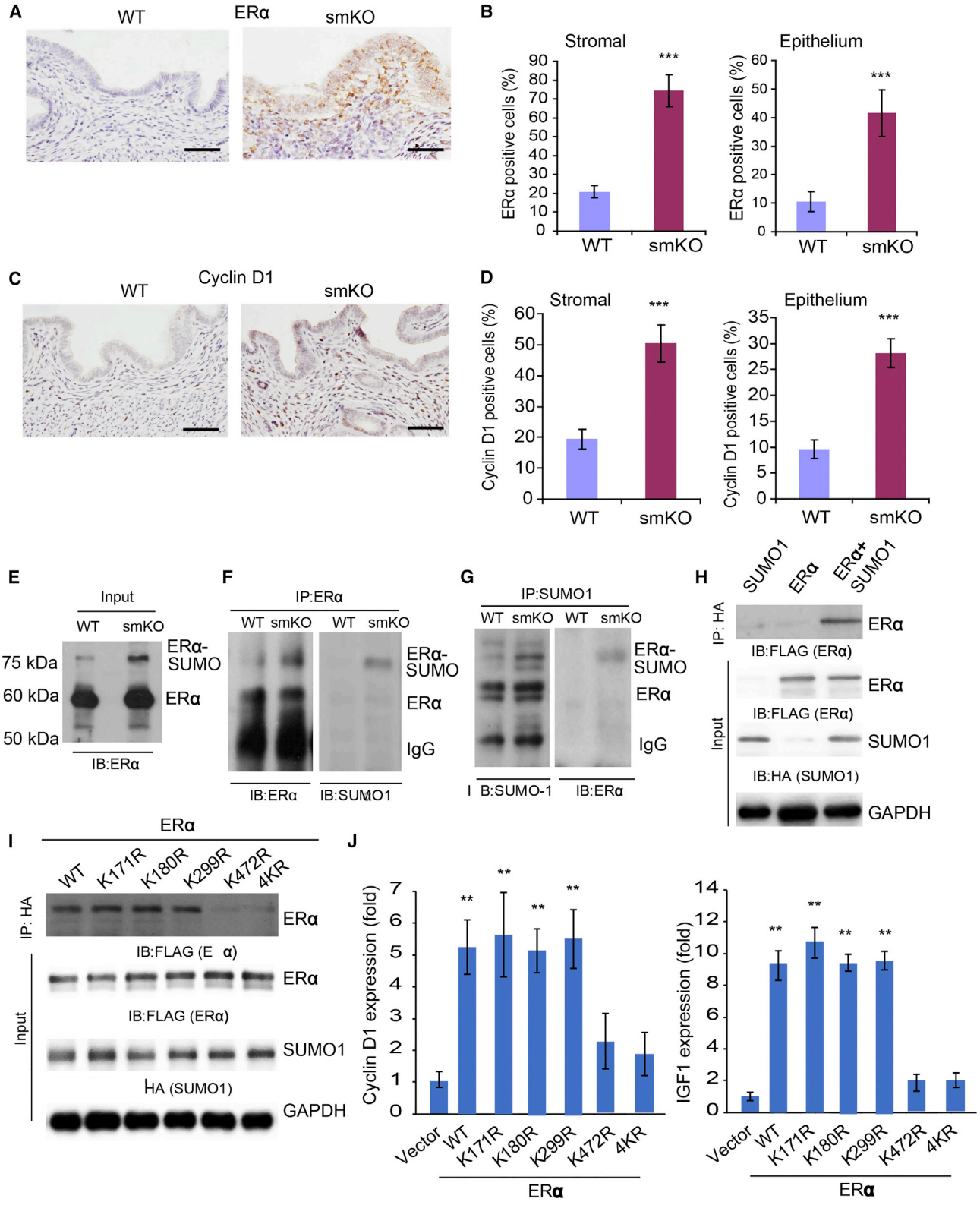

Figure 6. ERα SUMOylation at lys472 Augments Its Transcriptional Activity

(A and B) Immunohistochemical staining (A) and quantification (B) of ERα in uterine stroma and epithelium from 2-month-old WT and SENP1smKO mice.

(C) Immunohistochemical staining of cyclin D1 in uterine sections from 4-month-old WT and SENP1smKO mice.

(legend continued on next page)

progenitor cells; $CD34^+KLF4^+$ progenitor cells proliferate before migrating to the epithelial layer, where they transdifferentiate into epithelial cells, enhancing endometrial regeneration. Downregulation or loss of SENP1 induces SUMOylation and overactivation of ERα, which drives its own expression and augments estrogen-independent endometrial regeneration and, eventually, uterine hyperplasia with possible cancer progression. Of note, the Senp1 gene promoter contains the hypoxia response element (HRE), and SENP1 expression can be regulated in response to hypoxia (Xu et al., 2010). Recent studies suggest that dynamic spatial and temporal changes in hypoxia are involved in endometrial breakdown and repair (Cousins et al., 2016), and SENP1 expression should be tightly regulated by hypoxia in the endometrium. Therefore, in a normal menstrual cycle, in which SENP1 is turned on and off, the endometrium is exposed to a risk of cancer every time it undergoes normal repair throughout life. However, the exact mechanism leading to SENP1 depletion during endometrial regeneration in the mouse model remains unclear and will be further investigated in future studies, as will its relevance to human tissues.

Phenotypic markers specific to endometrial stem cells are being studied and have not yet been definitively characterized (Gurung et al., 2015). It has been reported that $CD146^+PDGFR\beta^+$ (platelet-derived growth factor receptor β positive) cells in the basalis and functionalis of the human endometrium localize to perivascular areas. Moreover, isolated stromal $CD146^+PDGFR\beta^+$ cells exhibit phenotypic and functional properties of MSCs, capable of differentiation into adipogenic, osteogenic, myogenic, and chondrogenic lineages (Schwab et al., 2005). The origin of endometrial stem cells has recently been examined by a phylogenetic approach by using RNA sequencing (RNA-seq) data to infer lineage relations among different cell types and to trace the pattern of gene-expression changes on a tree-like relation of cell types. This approach identified well-known regulators of the endometrium such as progesterone receptor (PGR) and FOXO1, as well as GATA2 as a potential stromal regulator, and is essential for endometrial stromal cell differentiation *in vitro* (Kin et al., 2015). Of note, GATA2 is a critical factor for vascular development and vascular remodeling in adults in our previous studies (Qiu et al., 2017; Yu et al., 2010). However, how the vascular $GATA2^+$ and perivascular $CD146^+PDGFR\beta^+$ cells contribute to cyclic regeneration of the endometrium needs to be determined. More important, our study on perivascular $CD34^+KLF4^+$ cells, together with these reports on stromal $CD146(MCAM)^+PDGFR\beta^+$ cells, may support a general theme by which resident perivascular cells function as the source of endometrial stem cells. CD146/MCAM (also known as the melanoma cell adhesion molecule or cell surface glycoprotein Muc18) functions as a receptor for laminin α4, a matrix molecule that is broadly expressed within the vascular wall (Flanagan et al., 2012). Accordingly, MCAM is highly expressed by cells that are components of the blood vessel wall, including vascular endothelial cells, SMCs, and pericytes. PDGFRβ is essential for the vascular development of pericytes and vascular SMCs, and therefore the integrity and/or functionality of the vasculature in multiple organs (Lindahl et al., 1997, 1998). It is worth determining whether the $CD34^+KLF4^+$ and $CD146(MCAM)^+PDGFR\beta^+$ cells are identical populations in the stroma and whether they are functionally equivalent during endometrial regeneration.

Adult tissue stem or progenitor cells not only express distinct cellular markers but also have a different chromatin landscape from their progeny. Whole-transcriptome RNA-seq analysis and an assay for transposase-accessible chromatin using sequencing (ATAC-seq) have been applied to characterize gene expression programs and chromatin accessibilities of MSCs from various tissues. Both RNA-seq and ATAC-seq can successfully define the molecular signature of MSCs based on their tissue origins. However, clustering based on tissue origin is more accurate with chromatin accessibility signatures than with transcriptome profiles (Ho et al., 2018). It should be mentioned that chromatin remodeling also depends on critical transcriptional factors that are expressed in specific progenitor cells. For example, cardiac progenitor cells (CPCs) fate transitions with distinct open chromatin states critically depend on CPC-specific transcriptional factors ISL1 and NKX2-5 (Jia et al., 2018). Similarly, OCT4-SOX2-KLK4 expression could drive dynamic changes in chromatin states, shifting from open to closed and closed to open states within particular loci. The open to closed loci are largely composed of genes associated with a somatic fate, while the closed to open loci are associated with pluripotency (Li et al., 2017). Of note, KLF4 is upregulated in the uterine $CD34^+KLF4^+$ progenitor cells. In a future study, we will characterize the chromatin accessibility in the uterine $CD34^+KLF4^+$ progenitor cells compared to both $SM22\alpha^+$ stromal cells and differentiated endometrial epithelial cells.

Estrogen stimulation of the endometrium is the primary etiological factor associated with the development of endometrial hyperplasia and adenocarcinoma. We observe endometrial hyperplasia and even endometrial cancer in aged SENP1smKO mice. Previously in SENP1smKO mice, we have observed delayed oocyte growth and follicle maturation with reduced follicle

(D) Quantification of cyclin $D1^+$ cells in stroma and endometrium.

(E–G) Uteri from WT and SENP1smKO mice were collected, and tissue lysates were subjected to co-immunoprecipitation (coIP) assays, as indicated. Inputs (E), coIP with anti-ERα (F), and coIP with anti-SUMO1 (G), followed by western blot with anti-ERα or anti-SUMO1, as indicated. ERα and SUMOylated ERα are indicated.

(H) Expression plasmid for FLAG-tagged ERα was co-transfected with HA-tagged SUMO1 into human stromal cells, and ERα SUMOylation was determined by coIP with anti-HA, followed by western blotting with anti-FLAG (ERα).

(I) The K472R mutation diminishes ERα SUMOylation. FLAG-tagged ERα WT or a KR mutant (mutation at K171, K180, K299, K472, or all 4K residues) was co-transfected with HA-tagged SUMO1 into human endometrial stromal cells (HESCs) in which endogenous SENP1 was knocked down by SENP1 small interfering RNA (siRNA), and ERα SUMOylation was determined by coIP with anti-HA, followed by western blotting with anti-FLAG (ERα).

(J) SUMOylation enhances ERα transcriptional activity. ERα WT or a KR mutant was co-transfected into HESCs. Expression of ERα downstream genes cyclin D1 and IGF1 was determined by qRT-PCR.

All of the data are presented as means ± SEMs; n = 5; $^{**}p < 0.01$ (two-sided Student's t test).

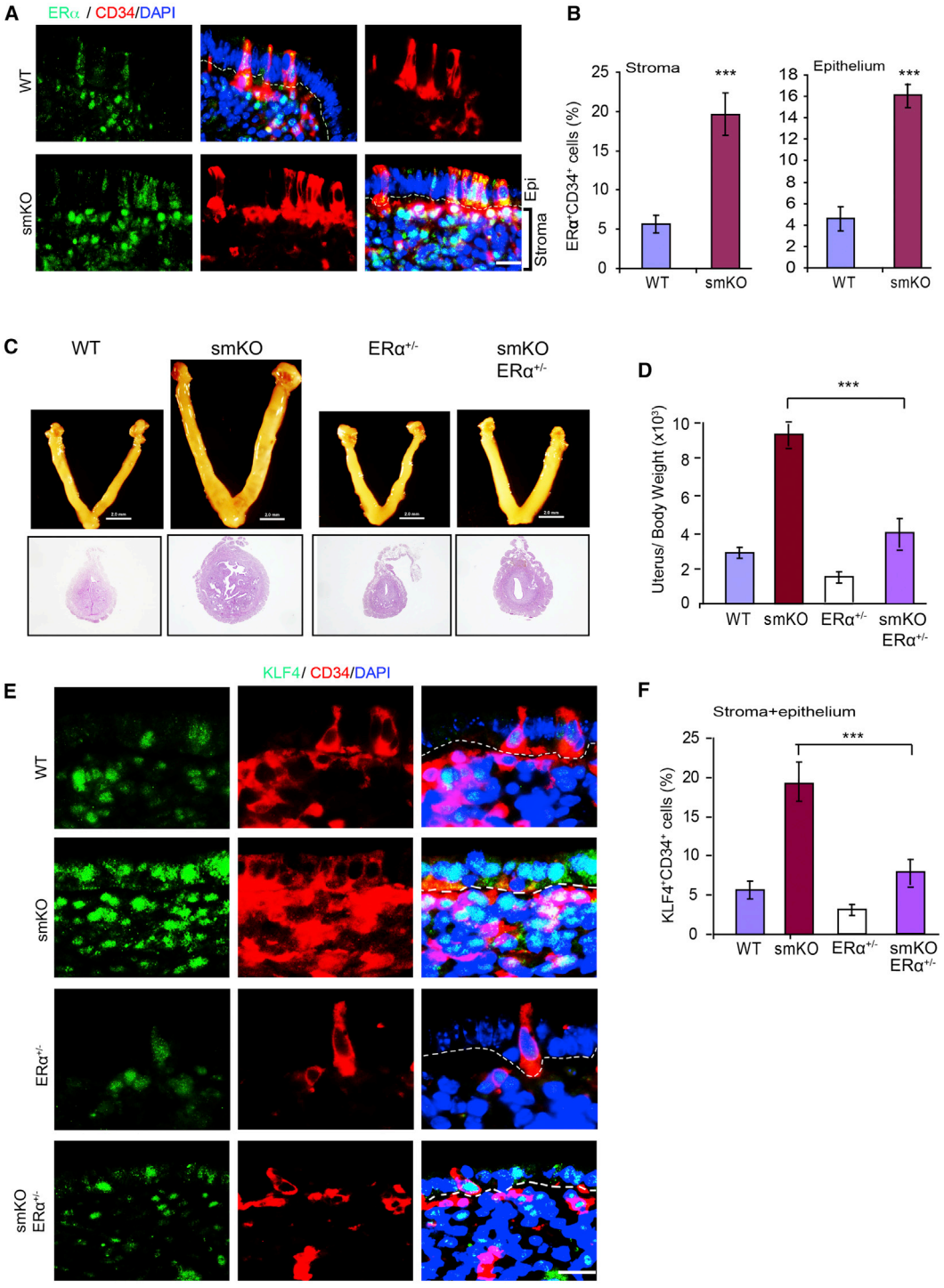

Figure 7. ERα Mediates Stem Cell Proliferation and Uterine Hyperplasia in SENP1smKO Mice

(A and B) Co-immunofluorescent staining (A) and quantification (B) of ERα and CD34 in uterine sections of 9-month-old WT and SENP1smKO mice. Representative images and quantifications of isolated uteri from WT and SENP1smKO mice at the age of 9 months.

(C and D) Representative images (C) and the ratios (D) of isolated uterus over body weight in WT, SENP1smKO, ERα$^{+/-}$ and SENP1smKO:ERα$^{+/-}$ mice at the age of 9 months.

(E and F) Co-immunofluorescent staining (E) and quantification (F) of KLF4 and CD34 in uterine sections of 9-month-old WT, SENP1smKO, ERα$^{+/-}$ and SENP1smKO:ERα$^{+/-}$ mice. Representative images and quantifications of isolated uteri from WT and SENP1smKO mice at the age of 9 months.

Scale bars: 20 μm (A and E) and 2.0 mm (C).

number and size during early oocyte development, leading to premature ovarian failure in late stages of ovulating life (Tan et al., 2017). However, here, we demonstrate that estradiol can stimulate endometrial hyperplasia in ovariectomized SENP1smKO mice, eliminating the possibility that these effects derive from the ovary. Our mutagenesis data support that augmented ERα activation by SUMO modification is critical for the described phenotype, as confirmed by showing that the ERα deletion completely blunts endometrial hyperplasia and cancer. Mechanistic studies suggest that the SUMOylation of ERα augments ERα transcriptional activity and downstream proliferative signaling in SM22α$^+$CD34$^+$KLF4$^+$ stem cells. Nevertheless, the potential role in endometrial regeneration of other SUMO targets besides ERα remains to be explored. It is well documented that the uncontrolled proliferation of stem cells leads to cancer (Jiang et al., 2017; Jones et al., 2006; Kota et al., 2017; Sahin et al., 2014; Wu et al., 2012; Yang et al., 2012; Zheng et al., 2015). Endometrial cancer is the most common cancer of the female reproductive system. Approximately 60,050 cases of endometrial cancer occur in the United States each year, which is more than the incidence of ovarian cancer and cervical cancer combined. Our study suggests that targeting ERα SUMOylation-dependent proliferation of stromal CD34$^+$KLF4$^+$ stem cells may provide a beneficial strategy for reducing the risk of endometrial cancer.

STAR★METHODS

Detailed methods are provided in the online version of this paper and include the following:

- KEY RESOURCES TABLE
- CONTACT FOR REAGENT AND RESOURCE SHARING
- EXPERIMENTAL MODEL AND SUBJECT DETAILS
  - Study approval
  - Smooth muscle 22α (SM22α) specific SENP1 knockout mice and tomato reporter mice
  - Rescue of uterine hyperplastic phenotype in SENP1smKO mice by deletion of estrogen receptor-α (ERα)
  - Mouse model of menstruation and treatment regimens
- METHOD DETAILS
  - Immunohistochemical Staining
  - Immunofluorescence staining
  - Quantitative PCR (qRT-PCR)
  - 3D co-culture system of endometrial formation (Arnold et al., 2001, 2002)
- QUANTIFICATION AND STATISTICAL ANALYSIS

SUPPLEMENTAL INFORMATION

Supplemental Information can be found online at https://doi.org/10.1016/j.celrep.2019.04.088.

ACKNOWLEDGMENTS

This work was supported by the National Key Research and Development Program of China (2016YFC1300600), the National Natural Science Foundation of China (U1601219), and Scientific Grants of Guangdong and Guangzhou (nos. 2015B020225002 and 201604020131). This work was supported by NIH grants HL136507, HL115148, and R01 HL109420. H.J.Z. is supported by a National Career Development Award from the American Heart Association (19CDA34760284). We appreciate Al Mennone's help in acquiring images in the Yale University Center for Cellular and Molecular Imaging (CCMI).

AUTHOR CONTRIBUTIONS

M.Y., H.J.Z., C.L., L.L., H.Z., and W.M. designed and performed the experiments and analyzed the data. M.Y. and W.M. wrote the manuscript. H.T. discussed the work and edited the manuscript.

DECLARATION OF INTERESTS

The authors declare no competing interests.

Received: August 28, 2018
Revised: March 1, 2019
Accepted: April 16, 2019
Published: May 28, 2019

REFERENCES

Arango, N.A., Kobayashi, A., Wang, Y., Jamin, S.P., Lee, H.H., Orvis, G.D., and Behringer, R.R. (2008). A mesenchymal perspective of Müllerian duct differentiation and regression in Amhr2-lacZ mice. Mol. Reprod. Dev. *75*, 1154–1162.

Arnold, J.T., Kaufman, D.G., Seppälä, M., and Lessey, B.A. (2001). Endometrial stromal cells regulate epithelial cell growth in vitro: a new co-culture model. Hum. Reprod. *16*, 836–845.

Arnold, J.T., Lessey, B.A., Seppälä, M., and Kaufman, D.G. (2002). Effect of normal endometrial stroma on growth and differentiation in Ishikawa endometrial adenocarcinoma cells. Cancer Res. *62*, 79–88.

Baarends, W.M., van Helmond, M.J., Post, M., van der Schoot, P.J., Hoogerbrugge, J.W., de Winter, J.P., Uilenbroek, J.T., Karels, B., Wilming, L.G., Meijers, J.H., et al. (1994). A novel member of the transmembrane serine/threonine kinase receptor family is specifically expressed in the gonads and in mesenchymal cells adjacent to the müllerian duct. Development *120*, 189–197.

Bentz, E.K., Kenning, M., Schneeberger, C., Kolbus, A., Huber, J.C., Hefler, L.A., and Tempfer, C.B. (2010). OCT-4 expression in follicular and luteal phase endometrium: a pilot study. Reprod. Biol. Endocrinol. *8*, 38.

Bilyk, O., Coatham, M., Jewer, M., and Postovit, L.M. (2017). Epithelial-to-Mesenchymal Transition in the Female Reproductive Tract: From Normal Functioning to Disease Pathology. Front. Oncol. *7*, 145.

Brasted, M., White, C.A., Kennedy, T.G., and Salamonsen, L.A. (2003). Mimicking the events of menstruation in the murine uterus. Biol. Reprod. *69*, 1273–1280.

Chan, R.W., Schwab, K.E., and Gargett, C.E. (2004). Clonogenicity of human endometrial epithelial and stromal cells. Biol. Reprod. *70*, 1738–1750.

Cheng, J., Kang, X., Zhang, S., and Yeh, E.T. (2007). SUMO-specific protease 1 is essential for stabilization of HIF1alpha during hypoxia. Cell *131*, 584–595.

Cherepanova, O.A., Gomez, D., Shankman, L.S., Swiatlowska, P., Williams, J., Sarmento, O.F., Alencar, G.F., Hess, D.L., Bevard, M.H., Greene, E.S., et al. (2016). Activation of the pluripotency factor OCT4 in smooth muscle cells is atheroprotective. Nat. Med. *22*, 657–665.

Cho, N.H., Park, Y.K., Kim, Y.T., Yang, H., and Kim, S.K. (2004). Lifetime expression of stem cell markers in the uterine endometrium. Fertil. Steril. *81*, 403–407.

Cousins, F.L., Murray, A.A., Scanlon, J.P., and Saunders, P.T. (2016). Hypoxyprobe™ reveals dynamic spatial and temporal changes in hypoxia in a mouse model of endometrial breakdown and repair. BMC Res. Notes *9*, 30.

Du, H., and Taylor, H.S. (2007). Contribution of bone marrow-derived stem cells to endometrium and endometriosis. Stem Cells *25*, 2082–2086.

Du, L., Li, Y.J., Fakih, M., Wiatrek, R.L., Duldulao, M., Chen, Z., Chu, P., Garcia-Aguilar, J., and Chen, Y. (2016). Role of SUMO activating enzyme in cancer stem cell maintenance and self-renewal. Nat. Commun. *7*, 12326.

Dupont, S., Krust, A., Gansmuller, A., Dierich, A., Chambon, P., and Mark, M. (2000). Effect of single and compound knockouts of estrogen receptors alpha (ERalpha) and beta (ERbeta) on mouse reproductive phenotypes. Development *127*, 4277–4291.

Edery, M., Mills, K.T., and Bern, H.A. (1989). Effects of testosterone on morphology and on progestin and estrogen receptor levels in the mouse uterus and mammary gland. Biol. Neonate *56*, 324–331.

Figueira, P.G., Abrão, M.S., Krikun, G., and Taylor, H.S. (2011). Stem cells in endometrium and their role in the pathogenesis of endometriosis. Ann. N.Y. Acad. Sci. *1221*, 10–17.

Flanagan, K., Fitzgerald, K., Baker, J., Regnstrom, K., Gardai, S., Bard, F., Mocci, S., Seto, P., You, M., Larochelle, C., et al. (2012). Laminin-411 is a vascular ligand for MCAM and facilitates TH17 cell entry into the CNS. PLoS One *7*, e40443.

Gargett, C.E. (2004). Stem cells in gynaecology. Aust. N.Z. J. Obstet. Gynaecol. *44*, 380–386.

Gargett, C.E. (2007). Uterine stem cells: what is the evidence? Hum. Reprod. Update *13*, 87–101.

Gargett, C.E., Schwab, K.E., Brosens, J.J., Puttemans, P., Benagiano, G., and Brosens, I. (2014). Potential role of endometrial stem/progenitor cells in the pathogenesis of early-onset endometriosis. Mol. Hum. Reprod. *20*, 591–598.

Gill, G. (2004). SUMO and ubiquitin in the nucleus: different functions, similar mechanisms? Genes Dev. *18*, 2046–2059.

Götte, M., Wolf, M., Staebler, A., Buchweitz, O., Kelsch, R., Schüring, A.N., and Kiesel, L. (2008). Increased expression of the adult stem cell marker Musashi-1 in endometriosis and endometrial carcinoma. J. Pathol. *215*, 317–329.

Gurung, S., Deane, J.A., Masuda, H., Maruyama, T., and Gargett, C.E. (2015). Stem Cells in Endometrial Physiology. Semin. Reprod. Med. *33*, 326–332.

Heldring, N., Pike, A., Andersson, S., Matthews, J., Cheng, G., Hartman, J., Tujague, M., Ström, A., Treuter, E., Warner, M., and Gustafsson, J.A. (2007). Estrogen receptors: how do they signal and what are their targets. Physiol. Rev. *87*, 905–931.

Hilmi, K., Hussein, N., Mendoza-Sanchez, R., El-Ezzy, M., Ismail, H., Durette, C., Bail, M., Rozendaal, M.J., Bouvier, M., Thibault, P., et al. (2012). Role of SUMOylation in full antiestrogenicity. Mol. Cell. Biol. *32*, 3823–3837.

Ho, Y.T., Shimbo, T., Wijaya, E., Ouchi, Y., Takaki, E., Yamamoto, R., Kikuchi, Y., Kaneda, Y., and Tamai, K. (2018). Chromatin accessibility identifies diversity in mesenchymal stem cells from different tissue origins. Sci. Rep. *8*, 17765.

Huang, C.C., Orvis, G.D., Wang, Y., and Behringer, R.R. (2012). Stromal-to-epithelial transition during postpartum endometrial regeneration. PLoS One *7*, e44285.

Jia, G., Preussner, J., Chen, X., Guenther, S., Yuan, X., Yekelchyk, M., Kuenne, C., Looso, M., Zhou, Y., Teichmann, S., and Braun, T. (2018). Single cell RNA-seq and ATAC-seq analysis of cardiac progenitor cell transition states and lineage settlement. Nat. Commun. *9*, 4877.

Jiang, R., Ding, L., Zhou, J., Huang, C., Zhang, Q., Jiang, Y., Liu, J., Yan, Q., Zhen, X., Sun, J., et al. (2017). Enhanced HOXA10 sumoylation inhibits embryo implantation in women with recurrent implantation failure. Cell Death Discov. *3*, 17057.

Jones, M.C., Fusi, L., Higham, J.H., Abdel-Hafiz, H., Horwitz, K.B., Lam, E.W., and Brosens, J.J. (2006). Regulation of the SUMO pathway sensitizes differentiating human endometrial stromal cells to progesterone. Proc. Natl. Acad. Sci. USA *103*, 16272–16277.

Kalluri, R., and Weinberg, R.A. (2009). The basics of epithelial-mesenchymal transition. J. Clin. Invest. *119*, 1420–1428.

Kato, K., Yoshimoto, M., Kato, K., Adachi, S., Yamayoshi, A., Arima, T., Asanoma, K., Kyo, S., Nakahata, T., and Wake, N. (2007). Characterization of side-population cells in human normal endometrium. Hum. Reprod. *22*, 1214–1223.

Kim, J.Y., Tavaré, S., and Shibata, D. (2005). Counting human somatic cell replications: methylation mirrors endometrial stem cell divisions. Proc. Natl. Acad. Sci. USA *102*, 17739–17744.

Kin, K., Nnamani, M.C., Lynch, V.J., Michaelides, E., and Wagner, G.P. (2015). Cell-type phylogenetics and the origin of endometrial stromal cells. Cell Rep. *10*, 1398–1409.

Kota, V., Sommer, G., Hazard, E.S., Hardiman, G., Twiss, J.L., and Heise, T. (2017). SUMO-modification of RNA-binding protein La regulates cell proliferation and STAT3 protein stability. Mol. Cell. Biol. *38*, e00129-17.

Kretzschmar, K., and Watt, F.M. (2012). Lineage tracing. Cell *148*, 33–45.

Lepore, J.J., Cheng, L., Min Lu, M., Mericko, P.A., Morrisey, E.E., and Parmacek, M.S. (2005). High-efficiency somatic mutagenesis in smooth muscle cells and cardiac myocytes in SM22alpha-Cre transgenic mice. Genesis *41*, 179–184.

Li, D., Liu, J., Yang, X., Zhou, C., Guo, J., Wu, C., Qin, Y., Guo, L., He, J., Yu, S., et al. (2017). Chromatin Accessibility Dynamics during iPSC Reprogramming. Cell Stem Cell *21*, 819–833.e6.

Lindahl, P., Johansson, B.R., Levéen, P., and Betsholtz, C. (1997). Pericyte loss and microaneurysm formation in PDGF-B-deficient mice. Science *277*, 242–245.

Lindahl, P., Hellström, M., Kalén, M., Karlsson, L., Pekny, M., Pekna, M., Soriano, P., and Betsholtz, C. (1998). Paracrine PDGF-B/PDGF-Rbeta signaling controls mesangial cell development in kidney glomeruli. Development *125*, 3313–3322.

Lynch, L., Golden-Mason, L., Eogan, M., O'Herlihy, C., and O'Farrelly, C. (2007). Cells with haematopoietic stem cell phenotype in adult human endometrium: relevance to infertility? Hum. Reprod. *22*, 919–926.

Majesky, M.W., Horita, H., Ostriker, A., Lu, S., Regan, J.N., Bagchi, A., Dong, X.R., Poczobutt, J., Nemenoff, R.A., and Weiser-Evans, M.C. (2017). Differentiated Smooth Muscle Cells Generate a Subpopulation of Resident Vascular Progenitor Cells in the Adventitia Regulated by Klf4. Circ. Res. *120*, 296–311.

Masuda, H., Matsuzaki, Y., Hiratsu, E., Ono, M., Nagashima, T., Kajitani, T., Arase, T., Oda, H., Uchida, H., Asada, H., et al. (2010). Stem cell-like properties of the endometrial side population: implication in endometrial regeneration. PLoS One *5*, e10387.

Matthai, C., Horvat, R., Noe, M., Nagele, F., Radjabi, A., van Trotsenburg, M., Huber, J., and Kolbus, A. (2006). Oct-4 expression in human endometrium. Mol. Hum. Reprod. *12*, 7–10.

Morelli, S.S., Yi, P., and Goldsmith, L.T. (2012). Endometrial stem cells and reproduction. Obstet. Gynecol. Int. *2012*, 851367.

Müller, S., Hoege, C., Pyrowolakis, G., and Jentsch, S. (2001). SUMO, ubiquitin's mysterious cousin. Nat. Rev. Mol. Cell Biol. *2*, 202–210.

Nephew, K.P., Long, X., Osborne, E., Burke, K.A., Ahluwalia, A., and Bigsby, R.M. (2000). Effect of estradiol on estrogen receptor expression in rat uterine cell types. Biol. Reprod. *62*, 168–177.

Ong, Y.R., Cousins, F.L., Yang, X., Mushafi, A.A.A.A., Breault, D.T., Gargett, C.E., and Deane, J.A. (2018). Bone Marrow Stem Cells Do Not Contribute to Endometrial Cell Lineages in Chimeric Mouse Models. Stem Cells *36*, 91–102.

Parasar, P., Sacha, C.R., Ng, N., McGuirk, E.R., Chinthala, S., Ozcan, P., Lindsey, J., Salas, S., Laufer, M.R., Missmer, S.A., and Anchan, R.M. (2017). Differentiating mouse embryonic stem cells express markers of human endometrium. Reprod. Biol. Endocrinol. *15*, 52.

Pattabiraman, D.R., and Weinberg, R.A. (2014). Tackling the cancer stem cells - what challenges do they pose? Nat. Rev. Drug Discov. *13*, 497–512.

Patterson, A.L., Zhang, L., Arango, N.A., Teixeira, J., and Pru, J.K. (2013). Mesenchymal-to-epithelial transition contributes to endometrial regeneration following natural and artificial decidualization. Stem Cells Dev. *22*, 964–974.

Pickart, C.M. (2001). Mechanisms underlying ubiquitination. Annu. Rev. Biochem. *70*, 503–533.

Qiu, C., Wang, Y., Zhao, H., Qin, L., Shi, Y., Zhu, X., Song, L., Zhou, X., Chen, J., Zhou, H., et al. (2017). The critical role of SENP1-mediated GATA2

deSUMOylation in promoting endothelial activation in graft arteriosclerosis. Nat. Commun. *8*, 15426.

Sahin, U., Ferhi, O., Carnec, X., Zamborlini, A., Peres, L., Jollivet, F., Vitaliano-Prunier, A., de Thé, H., and Lallemand-Breitenbach, V. (2014). Interferon controls SUMO availability via the Lin28 and let-7 axis to impede virus replication. Nat. Commun. *5*, 4187.

Saitoh, H., and Hinchey, J. (2000). Functional heterogeneity of small ubiquitin-related protein modifiers SUMO-1 versus SUMO-2/3. J. Biol. Chem. *275*, 6252–6258.

Schwab, K.E., Chan, R.W., and Gargett, C.E. (2005). Putative stem cell activity of human endometrial epithelial and stromal cells during the menstrual cycle. Fertil. Steril. *84* (*Suppl 2*), 1124–1130.

Shankman, L.S., Gomez, D., Cherepanova, O.A., Salmon, M., Alencar, G.F., Haskins, R.M., Swiatlowska, P., Newman, A.A., Greene, E.S., Straub, A.C., et al. (2015). KLF4-dependent phenotypic modulation of smooth muscle cells has a key role in atherosclerotic plaque pathogenesis. Nat. Med. *21*, 628–637.

Shao, L., Zhou, H.J., Zhang, H., Qin, L., Hwa, J., Yun, Z., Ji, W., and Min, W. (2015). SENP1-mediated NEMO deSUMOylation in adipocytes limits inflammatory responses and type-1 diabetes progression. Nat. Commun. *6*, 8917.

Sidney, L.E., Branch, M.J., Dunphy, S.E., Dua, H.S., and Hopkinson, A. (2014). Concise review: evidence for CD34 as a common marker for diverse progenitors. Stem Cells *32*, 1380–1389.

Solway, J., Seltzer, J., Samaha, F.F., Kim, S., Alger, L.E., Niu, Q., Morrisey, E.E., Ip, H.S., and Parmacek, M.S. (1995). Structure and expression of a smooth muscle cell-specific gene, SM22 alpha. J. Biol. Chem. *270*, 13460–13469.

Spencer, T.E., Hayashi, K., Hu, J., and Carpenter, K.D. (2005). Comparative developmental biology of the mammalian uterus. Curr. Top. Dev. Biol. *68*, 85–122.

Suzuki, A., Urushitani, H., Watanabe, H., Sato, T., Iguchi, T., Kobayashi, T., and Ohta, Y. (2007). Comparison of estrogen responsive genes in the mouse uterus, vagina and mammary gland. J. Vet. Med. Sci. *69*, 725–731.

Takahashi, K., and Yamanaka, S. (2016). A decade of transcription factor-mediated reprogramming to pluripotency. Nat. Rev. Mol. Cell Biol. *17*, 183–193.

Tan, S., Feng, B., Yin, M., Zhou, H.J., Lou, G., Ji, W., Li, Y., and Min, W. (2017). Stromal Senp1 promotes mouse early folliculogenesis by regulating BMP4 expression. Cell Biosci. *7*, 36.

Taylor, H.S. (2004). Endometrial cells derived from donor stem cells in bone marrow transplant recipients. JAMA *292*, 81–85.

Thiruvalluvan, M., Barghouth, P.G., Tsur, A., Broday, L., and Oviedo, N.J. (2018). SUMOylation controls stem cell proliferation and regional cell death through Hedgehog signaling in planarians. Cell. Mol. Life Sci. *75*, 1285–1301.

Wang, Y., Zhu, L., Kuokkanen, S., and Pollard, J.W. (2015). Activation of protein synthesis in mouse uterine epithelial cells by estradiol-17β is mediated by a PKC-ERK1/2-mTOR signaling pathway. Proc. Natl. Acad. Sci. USA *112*, E1382–E1391.

Wen, L., Wang, Y., Wen, N., Yuan, G., Wen, M., Zhang, L., Liu, Q., Liang, Y., Cai, C., Chen, X., and Ding, Y. (2016). Role of Endothelial Progenitor Cells in Maintaining Stemness and Enhancing Differentiation of Mesenchymal Stem Cells by Indirect Cell-Cell Interaction. Stem Cells Dev. *25*, 123–138.

Wolff, E.F., Wolff, A.B., Hongling Du, and Taylor, H.S. (2007). Demonstration of multipotent stem cells in the adult human endometrium by in vitro chondrogenesis. Reprod. Sci. *14*, 524–533.

Wu, Y., Guo, Z., Wu, H., Wang, X., Yang, L., Shi, X., Du, J., Tang, B., Li, W., Yang, L., and Zhang, Y. (2012). SUMOylation represses Nanog expression via modulating transcription factors Oct4 and Sox2. PLoS One *7*, e39606.

Xu, Y., Zuo, Y., Zhang, H., Kang, X., Yue, F., Yi, Z., Liu, M., Yeh, E.T., Chen, G., and Cheng, J. (2010). Induction of SENP1 in endothelial cells contributes to hypoxia-driven VEGF expression and angiogenesis. J. Biol. Chem. *285*, 36682–36688.

Yamashita, S., Newbold, R.R., McLachlan, J.A., and Korach, K.S. (1989). Developmental pattern of estrogen receptor expression in female mouse genital tracts. Endocrinology *125*, 2888–2896.

Yang, F., Yao, Y., Jiang, Y., Lu, L., Ma, Y., and Dai, W. (2012). Sumoylation is important for stability, subcellular localization, and transcriptional activity of SALL4, an essential stem cell transcription factor. J. Biol. Chem. *287*, 38600–38608.

Yeh, E.T. (2009). SUMOylation and De-SUMOylation: wrestling with life's processes. J. Biol. Chem. *284*, 8223–8227.

Yin, M., Li, X., Tan, S., Zhou, H.J., Ji, W., Bellone, S., Xu, X., Zhang, H., Santin, A.D., Lou, G., and Min, W. (2016). Tumor-associated macrophages drive spheroid formation during early transcoelomic metastasis of ovarian cancer. J. Clin. Invest. *126*, 4157–4173.

Yin, M., Zhou, H.J., Zhang, J., Lin, C., Li, H., Li, X., Li, Y., Zhang, H., Breckenridge, D.G., Ji, W., and Min, W. (2017). ASK1-dependent endothelial cell activation is critical in ovarian cancer growth and metastasis. JCI Insight *2*, 91828.

Yu, L., Ji, W., Zhang, H., Renda, M.J., He, Y., Lin, S., Cheng, E.C., Chen, H., Krause, D.S., and Min, W. (2010). SENP1-mediated GATA1 deSUMOylation is critical for definitive erythropoiesis. J. Exp. Med. *207*, 1183–1195.

Zheng, J., Liu, L., Wang, S., and Huang, X. (2015). SUMO-1 Promotes Ishikawa Cell Proliferation and Apoptosis in Endometrial Cancer by Increasing Sumoylation of Histone H4. Int. J. Gynecol. Cancer *25*, 1364–1368.

Zhou, H.J., Qin, L., Zhang, H., Tang, W., Ji, W., He, Y., Liang, X., Wang, Z., Yuan, Q., Vortmeyer, A., et al. (2016). Augmented endothelial exocytosis of angiopoietin-2 resulting from CCM3-deficiency contributes to the progression of cerebral cavernous malformation. Nat. Med. *22*, 1033–1042.

Zhu, X., Ding, S., Qiu, C., Shi, Y., Song, L., Wang, Y., Wang, Y., Li, J., Wang, Y., Sun, Y., et al. (2017). SUMOylation Negatively Regulates Angiogenesis by Targeting Endothelial NOTCH Signaling. Circ. Res. *121*, 636–649.

Zong, H., Espinosa, J.S., Su, H.H., Muzumdar, M.D., and Luo, L. (2005). Mosaic analysis with double markers in mice. Cell *121*, 479–492.

Zwijsen, R.M., Wientjens, E., Klompmaker, R., van der Sman, J., Bernards, R., and Michalides, R.J. (1997). CDK-independent activation of estrogen receptor by cyclin D1. Cell *88*, 405–415.

STAR★METHODS

KEY RESOURCES TABLE

REAGENT or RESOURCE	SOURCE	IDENTIFIER
Antibodies		
Rabbit polyclonal anti-SUMO1	Cell Signaling Technology	Cat#4930;RRID:AB_10698887
Rabbit monoclonal anti-SENP1	Abcam	Ab108981;RRID:AB_10862449
Rabbit polyclonal anti-KLF4	Abcam	ab129473; N/A
Got polyclonal anti-SM22-α	Abcam	ab10135;RRID:AB_2255631
Rabbit monoclonal anti-CD34	Abcam	ab81289;RRID:AB_1640331
Mouse monoclonal anti-E Cadherin	Abcam	Cat# ab76055, RRID:AB_1310159
Rabbit monoclonal anti-Estrogen Receptor alpha antibody	Abcam	Cat# ab108398, RRID:AB_10863604
Rabbit monoclonal anti-Ki67	Cell Signaling Technology	Cat# 9129, RRID:AB_2687446
Rabbit monoclonal anti-Desmin	Abcam	Cat# ab32362, RRID:AB_731901
Rabbit monoclonal anti-Oct4	Abcam	Cat# ab181557, RRID:AB_2687916
Mouse monoclonal anti-Cytokeratin 14	Abcam	Cat# ab7800, RRID:AB_306091
Rabbit monoclonal anti-Cyclin D1	Abcam	Cat# ab134175, RRID:AB_2750906
APC armenian hamstermonoclonal anti-mouse CD34 antibody	Biolegend	Cat# 128612, RRID:AB_10553896
PE mouse monoclonal antibody anti-OCT4 (OCT3)	Biolegend	Cat# 653703, RRID:AB_2562017
Bacterial and Virus Strains		
Clinical paraffin samples of human uterus	The First Affiliated Hospital, Sun Yat-sen University, Guangzhou, China	N/A
Chemicals, Peptides, and Recombinant Proteins		
β-Estradiol	Sigma-Aldrich	CAS: 50-28-2
Progesterone	Sigma-Aldrich	CAS: 57-83-0
Castor oil	Sigma-Aldrich	CAS:8001-79-4
3.3′-diaminobenzidine tetrahydrochloride	Sigma-Aldrich	CAS:D3939-1set
Experimental Models: Cell Lines		
Human endometrial stromal cells (HESCs)	Department of Gynaecology and Obstetrics, Yale University	https://medicine.yale.edu/obgyn/
Experimental Models: Organisms/Strains		
mT/mG reporter mice (ROSA-26Sor$^{tm4(ACTB-tdTomato,\ EGFP)Luo}$/J	The Jackson Laboratory	https://www.jax.org
Senp1$^{fl/fl}$ mice	Min lab	N/A
Oligonucleotides		
Primer: Sumo-1 Forward: ATTGGACAGGATAG CAGTGAGA	This paper	N/A
Primer: SENP1 Forward: CTGGGGAGGTGAC CTTAGTGA	This paper	N/A
Primer: CD34 Forward: AAGGCTGGGTGAAG ACCCTTA	This paper	N/A
Primer: KLF4 Forward: GTGCCCCGACTAA CCGTTG	This paper	N/A
Primer: GAPDH Forward: ACCACAGTCCAT GCCATCAC	This paper	N/A
Primer: AMHR2 Forward: GGGGCTTTGGA CACTGCTT	This paper	N/A
Primer: Cyclin D1 Forward: GCGTACCCT GACACCAATCTC	This paper	N/A

(*Continued on next page*)

Continued		
REAGENT or RESOURCE	SOURCE	IDENTIFIER
Primer: ERα Forward: CCCACTCAACAG CGTGTCTC	This paper	N/A
Primer: SM22α Forward: CAACAAGGGT CCATCCTACGG	This paper	N/A
Primer: DESMIN Forward: GTGGATGCA GCCACTCTAGC	This paper	N/A
Software and Algorithms		
Prism 4.0	GraphPad	https://www.graphpad.com/scientific-software/prism/
ImageJ		https://imagej.nih.gov/ij/
SAS software (version 9.1.4)	SAS Institute, Cary, NC	https://www.sas.com/geohome/html
MATLAB software	The Math Works, Inc. Natick, MA	https://www.mathworks.com

CONTACT FOR REAGENT AND RESOURCE SHARING

Reagents and all other data supporting the presented findings are available upon request to the Lead Contact, Wang Min (wang.min@yale.edu).

EXPERIMENTAL MODEL AND SUBJECT DETAILS

Study approval

All animal studies were approved by the Institutional Animal Care and Use Committee of Yale University. Use of clinical paraffin samples were approved by Institutional Review Board at The First Affiliated Hospital, Sun Yat-sen University, Guangzhou, China.

Smooth muscle 22α (SM22α) specific SENP1 knockout mice and tomato reporter mice

Senp1$^{fl/fl}$ mice were generated by inserting loxP sites surrounding the Senp1 gene exons 5 and 6, based on homologous recombination. Senp1$^{fl/fl}$ mice were mated with a deleter line carrying the Cre recombinase driven by the Sm22α-promoter (sm22α-Cre:B6.129S6-*Tagln*$^{tm2(cre)Yec}$/J purchased from the Jackson Laboratory)(Qiu et al., 2017; Shao et al., 2015; Tan et al., 2017; Yu et al., 2010; Zhu et al., 2017). For the reporter mice, the SM22α-Cre deleter mice were mated with mT/mG reporter mice (ROSA-26Sor$^{tm4(ACTB-tdTomato,\ EGFP)Luo}$/J; purchased from The Jackson Laboratory) to generate sm22α:mT/mG mice. In addition, we mated Senp1$^{fl/fl}$:sm22α-Cre (SENP1smKO) to mT/mG reporter mice to generate Senp1$^{fl/fl}$:sm22α-Cre:mT/mG (named Senp1smKO:mT/G mice). All mice had been subsequently backcrossed onto the C57BL/6 background for 6th generations. The deletion of SENP1 in uterine stromal cells of SENP1$^{fl/fl}$:Cre was verified by quantitative PCR with reverse transcription using primers amplifying exons 5–6 (Shao et al., 2015; Yu et al., 2010) and SENP1$^{+/+}$ & specific Cre or Senp1$^{fl/fl}$ mice used as controls. Mice were cared for in accordance with National Institutes of Health guidelines, and all procedures. All animal studies were approved by the Institutional Animal Care and Use Committee of Yale University.

Rescue of uterine hyperplastic phenotype in SENP1smKO mice by deletion of estrogen receptor-α (ERα)

ERα$^{+/-}$ mice obtained from Jackson Laboratory. All mice had been subsequently backcrossed onto the C57BL/6 background for 6th generations. SENP1smKO:ERα were obtained by mating SENP1smKO with ERα$^{+/-}$ mice. Senp1$^{fl/fl}$ and ERα$^{+/-}$ knockout mice were used as controls.

Mouse model of menstruation and treatment regimens

All mice in this study unless indicated were non-pregnant female mice at proestrous stage. One week after ovariectomy female C57BL/6 mice received s.c. injections of 100 ng 17-β-estradiol (E2, internal source) in ethanol/arachis oil (1:9) on three consecutive days. After three-days a progesterone (P4) releasing silastic tube (0.5 mg P4/d, internal source) was implanted s.c. into the back of mice followed by further applications of 10 ng E2 on three consecutive days. Concomitant with the last E2 treatment 50 μL sesame oil was injected into one uterus horn to induce decidualization (Brasted et al., 2003). The P4 implants were removed 48 h later. Mice were sacrificed at indicated points of time after steroid withdrawal and uteri were weighed and harvested for further analyses. All surgeries were performed under isoflurane-induced anesthesia.

METHOD DETAILS

Immunohistochemical Staining

Paraffin-embedded samples isolated from uterus of mouse or human were sectioned at a thickness of 4 μm. To stain SUMO1, SM22α, CD34, E-cadherin, keratin-14, KLF4 and ERα and cyclin D1, the slides were first deparaffinized in xylene and rehydrated with gradient concentrations of alcohol under standard procedures. After rehydration, the slides were immersed in 0.01 mol/L citrate buffer (pH 6.0) and heated (95°C) for 15 min for antigen retrieval. Then, the samples were incubated with 3% hydrogen peroxide (H_2O_2) for 10 minutes followed by 10% normal goat serum blocking for 10 minutes. Subsequently, the sections were incubated with primary antibody for overnight at 4°C. After washing with TBST for 3 times, the sections were incubated with biotin-labeled secondary antibody followed by horseradish peroxidase (HRP)-conjugated streptavidin for 30 minutes individually at room temperature. After applying HRP substrate, 3.3′-diaminobenzidine tetrahydrochloride (D3939-1set, Sigma) in 0.01% H_2O_2, for 2-10 minutes, the slides were counterstained with Meyer's hematoxylin for 30 to 60 s and mounted with mounting medium for visualization under microscope. (Yin et al., 2016; Yin et al., 2017). Scoring of SUMO1 and ERα in EC samples via IHC staining follows the methods previously published. All of IHC staining samples from EC patients were independently evaluated by experienced two pathologists.

Immunofluorescence staining

A respective isotype control was used in all of our immunostaining. For example, anti-CD34 antibody was a rabbit antibody (abcam) therefore a rabbit IgG isotype from abcam was used as a primary antibody control followed by the same secondary antibody (e.g., Alexa Fluor®-conjugated donkey anti-rabbit). Confocal microscopy images were taken with a Zeiss-LSM 700 microscope and evaluated using the ZEN2010 software. For mean fluorescence intensity measurements, confocal microscopy images were analyzed with ImageJ. Slides were observed using a Zeiss Axiovert 200 fluorescence microscope (Carl Zeiss MicroImaging; Thornwood, NY), and images were captured using Openlab3 software (Improvision, Lexington, MA). For tissue, 5 μm serial sections cut from frozen, OCT-embedded tissues were fixed in −20°C acetone for 10 minutes, dried for 15 minutes, followed by the same blocking/antibody protocol for cells as listed above. All images were taken at least from 4 areas of each section randomly and 5 sections per mice using a light microscope with 40x objective lens. Images were quantified using the MATLAB software (The Math Works, Inc. Natick, MA) as described previously (Zhou et al., 2016). The endometrium repairing zone was identified and both epithelium and stroma regions were marked using Photoshop. Number of target positive cells were counted and quantified as % of total $DAPI^+$ cells in the region.

Quantitative PCR (qRT-PCR)

Total RNA was extracted from human tissues using the RNeasy Plus Mini Kit (74134, QIAGEN), and then converted into cDNAs using the High Capacity cDNA Reverse Transcription Kit (4368814, Applied Biosystems) following the manufacturer's instruction. Quantitative PCR was performed with a CFX-96 (Bio-Rad) using the RT2 SYBR Green (330500, SA Biosciences). All values were normalized with GAPDH abundance. Data were presented as the average of triplicates ± SD.

3D co-culture system of endometrial formation (Arnold et al., 2001, 2002)

$GFP(SM22)^+CD34^+$ uterine stromal cells isolated from mT/mG reporter mice (WT) and SENP1smKO:mT/mG mice at age of 2-months. The 24-well plates were precoated with Matrigel and $SM22^+CD34^+$ uterine stromal cells (total cell number as $1*10^6$ cells / well) were directly seeded onto the matrigel-precoated 24 well plate. The cells were incubated at 37°C for up to 48 hours to allow endometrium to form. Starting hour 6 and 48, the cells fluorescent microscopic images to analyze the morphology. The well without cells but containing medium was used as negative control. All assays were performed at least three times and each time was tested in triplicate.

QUANTIFICATION AND STATISTICAL ANALYSIS

Group sizes were determined by an *a priori* power analysis for a two-tailed, two-sample t test with an α of 0.05 and power of 0.8, in order to detect a 10% difference in uterus hyperplasia and histological parameters (e.g., uterus weight and numbers of progenitor cells) at the endpoint. Female animals were grouped with no blinding but randomized during the experiments. No samples or animals were excluded from analysis. All quantifications (e.g., uterus weight, body weight, cytokines, apoptosis, progenitor cell populations, ERα activation) were performed in a blinded fashion. The differences of results of western-blot, qRT-PCR, immunostainings, FACS, and endometrium formation were analyzed by Student's t test. All figures are representative of at least three experiments unless otherwise noted. All graphs report mean ± SEM values of biological replicates. Comparisons between two groups were performed by paired t test, between more than two groups by one-way ANOVA followed by Bonferroni's post hoc test or by two-way ANOVA using Prism 4.0 software (GraphPad). P values were two-tailed and values < 0.05 were considered to indicate statistical significance. $p < 0.05$, $p < 0.01$ and $p < 0.001$ are designated in all figures unless specified with *, **, ***, respectively.

Cell Reports, Volume *27*

Supplemental Information

$CD34^{+}KLF4^{+}$ Stromal Stem Cells Contribute to Endometrial Regeneration and Repair

Mingzhu Yin, Huanjiao Jenny Zhou, Caixia Lin, Lingli Long, Xiaolei Yang, Haifeng Zhang, Hugh Taylor, and Wang Min

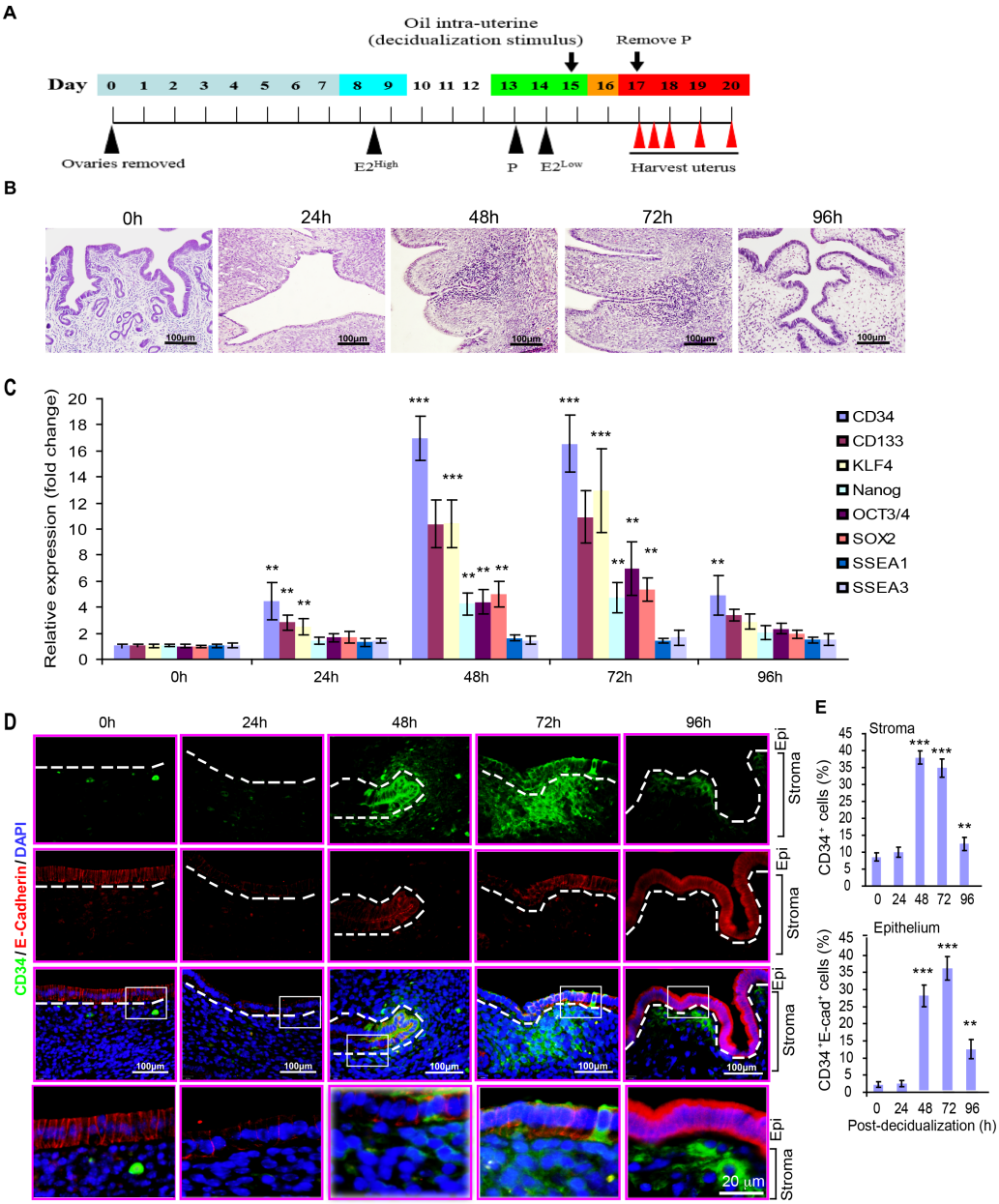

Figure S1. Stem cell markers expression increased in the process of endometrial self-repair. Related to Fig.1.

A. Establishment of mouse endometrial decidualization model. Ovariectomized mice were treated with estradiol (E2) injections and progesterone releasing implants to stimulate endometrial proliferation and differentiation. Decidualization was induced by injection of oil into one uterine cavity. Endometrial bleeding in response to removal of the progesterone implant was monitored by vaginal smears or blood collection with cotton pads. Uteri collected at 0, 24, 48, 72, and 96 hours post-progesterone (P4) withdrawal were used for histology and analysis of gene expression. **B**. Representative images of H&E staining for tissue sections from the mouse uterus. **C.** Mesenchymal stem cell markers were determined by qRT-PCR in mouse uterus. **D.** Immunofluorescent staining of CD34 and E-cadherin in tissue sections. An insert image with high magnification is shown underneath. **E.** Quantifications of $CD34^+$ cells in stroma, and of $CD34^+$E-$cadherin^+$ cells in the epithelium. All data are presented as means ± SEM, n=5, **, P<0.01; ***, P<0.001 (two-sided student's t-test). Scale bar: 100 μm (B,D).

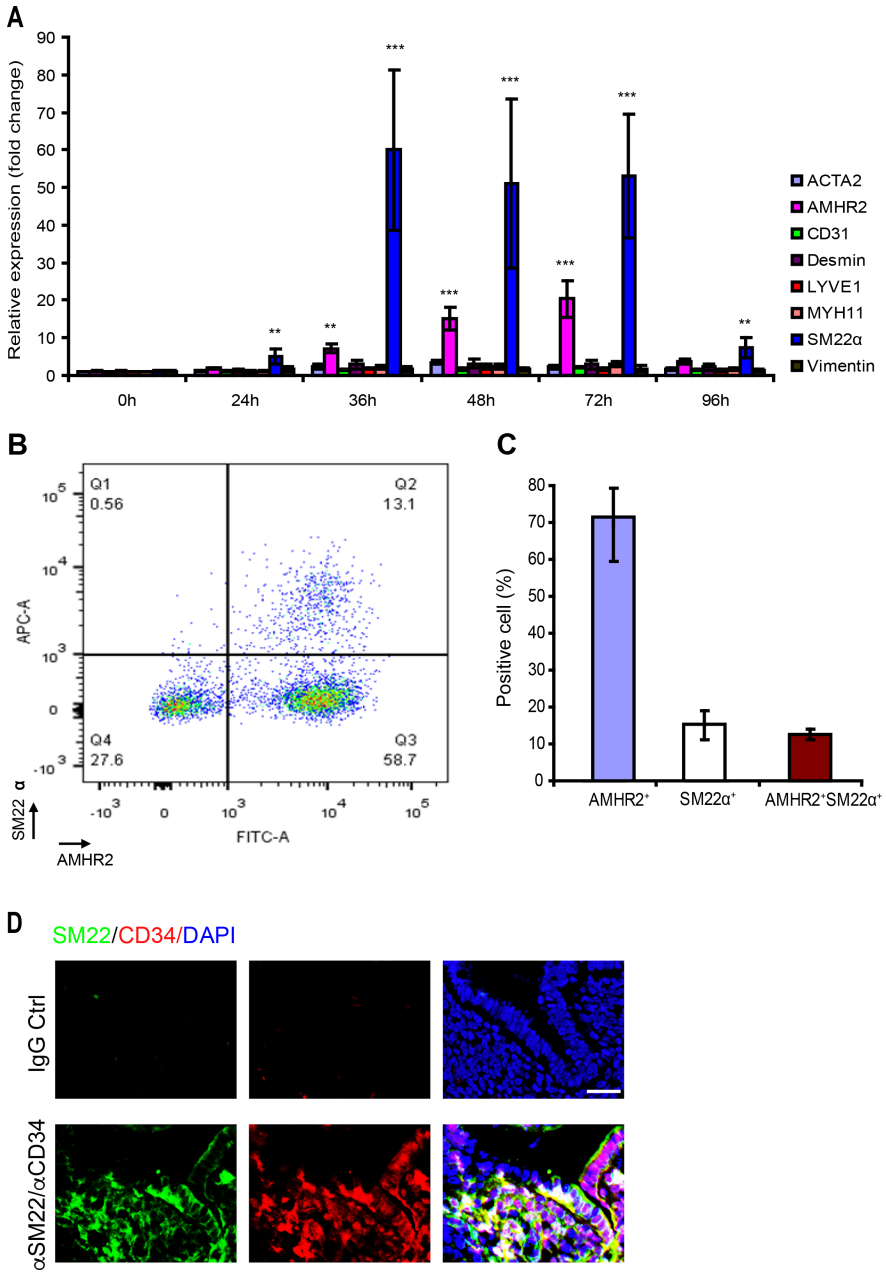

Figure S2. SM22α positive cells are increased during the repairing process of the mouse uterus post-injury. Related to Fig.1.

A. Uterine stromal markers were determined by qRT-PCR in mouse uterus at 0, 24, 36, 48, 72, and 96 hours post-injection of castor oil. All data are presented as means ± SEM, n=5, **, P<0.01; ***, P<0.001 (two-sided student's t-test). **B-C**. FACS analyses of AMHR2$^+$SM22α$^+$ stromal cells in uterine from 2-month old mice. A representative FACS is shown in B. % of AMHR2$^+$ and SM22α$^+$ stromal cells were quantified (C). **D**. Isotype controls for immunofluorescent staining of SM22α and CD34 in tissue sections of Fig.2A (72 h time point samples were used). An isotype control for anti-CD34 antibody (abcam rabbit) and anti-SM22α (abcam goat) were used as primary antibodies followed by secondary antibodies (donkey anti-rabbit and donkey anti-goat). 25 μm (D).

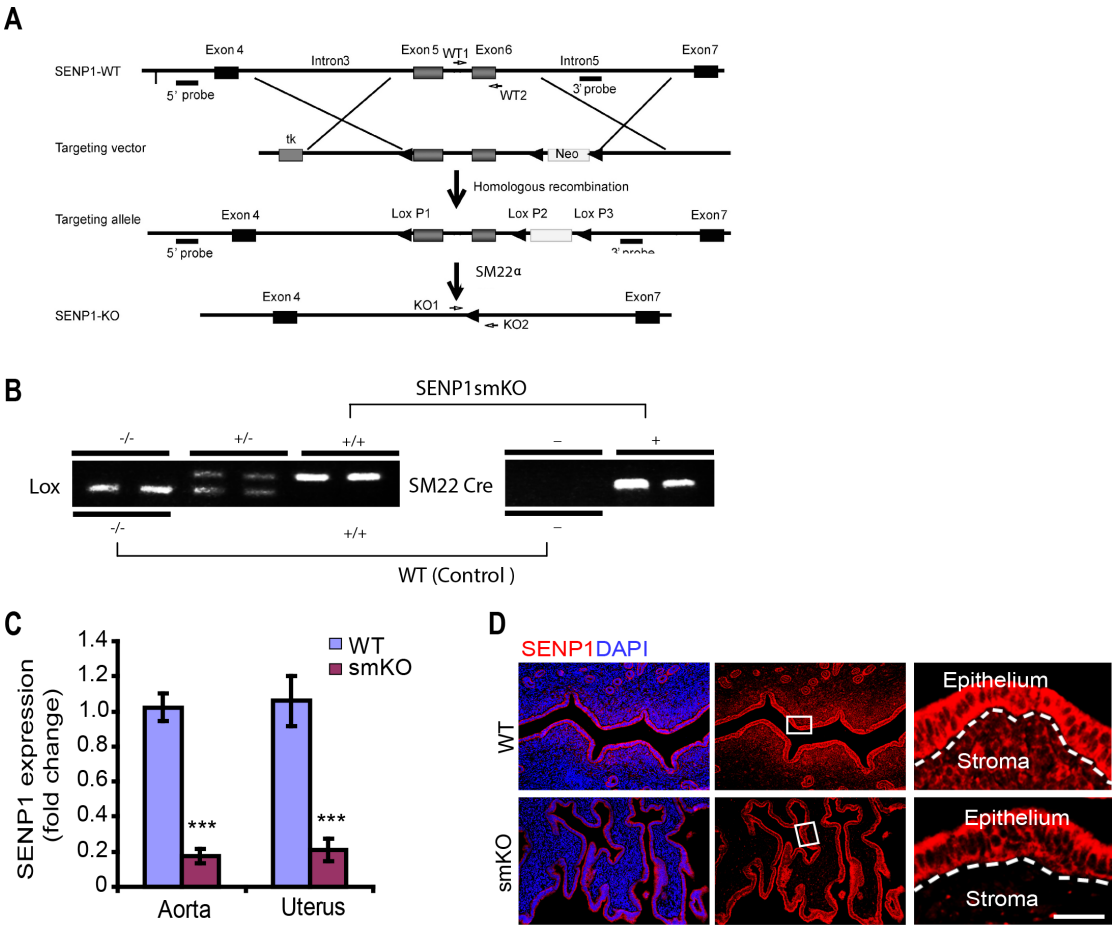

Figure S3. Specific deletion of SENP1 in smooth muscle of SENP1-deficient mice. Related to Fig.2.

A. SENP1$^{lox/lox}$ mice were generated based on homologous recombination. SENP1$^{lox/lox}$ mice were mated with SM22α Cre to obtain smooth muscle-specific SENP1-deficient (SENP1$^{lox/lox}$-SM22 Cre) mice.

B. Generation of SENP1$^{lox/lox}$ (WT) and SENP1$^{lox/lox}$-SM22Cre (SENP1smKO) mice. Tail genomic DNA was used to determine SENP1 deletion by PCR with KO primers adjacent to 5' of lox P1 (KO1) and lox P3 (KO2) to obtain heterozygous mice with a deletion of both the targeting region (the exons 5/6) and the Neo gene (SENP1$^{+/-}$). SENP1 KO mice were obtained by intercrossing between the heterozygous (SENP1$^{+/-}$) male and female. Representative genotypes are shown.

C. SENP1 was determined by qRT-PCR in uterus of WT and SENP1smKO mice at P21.

D. SENP1 deletion in the stroma, but not the epithelium layer of uterus. SENP1 was stained with anti-SENP1 antibody followed by DAPI counterstaining in uterus of WT and SENP1smKO mice at P21. 100 μm (D).

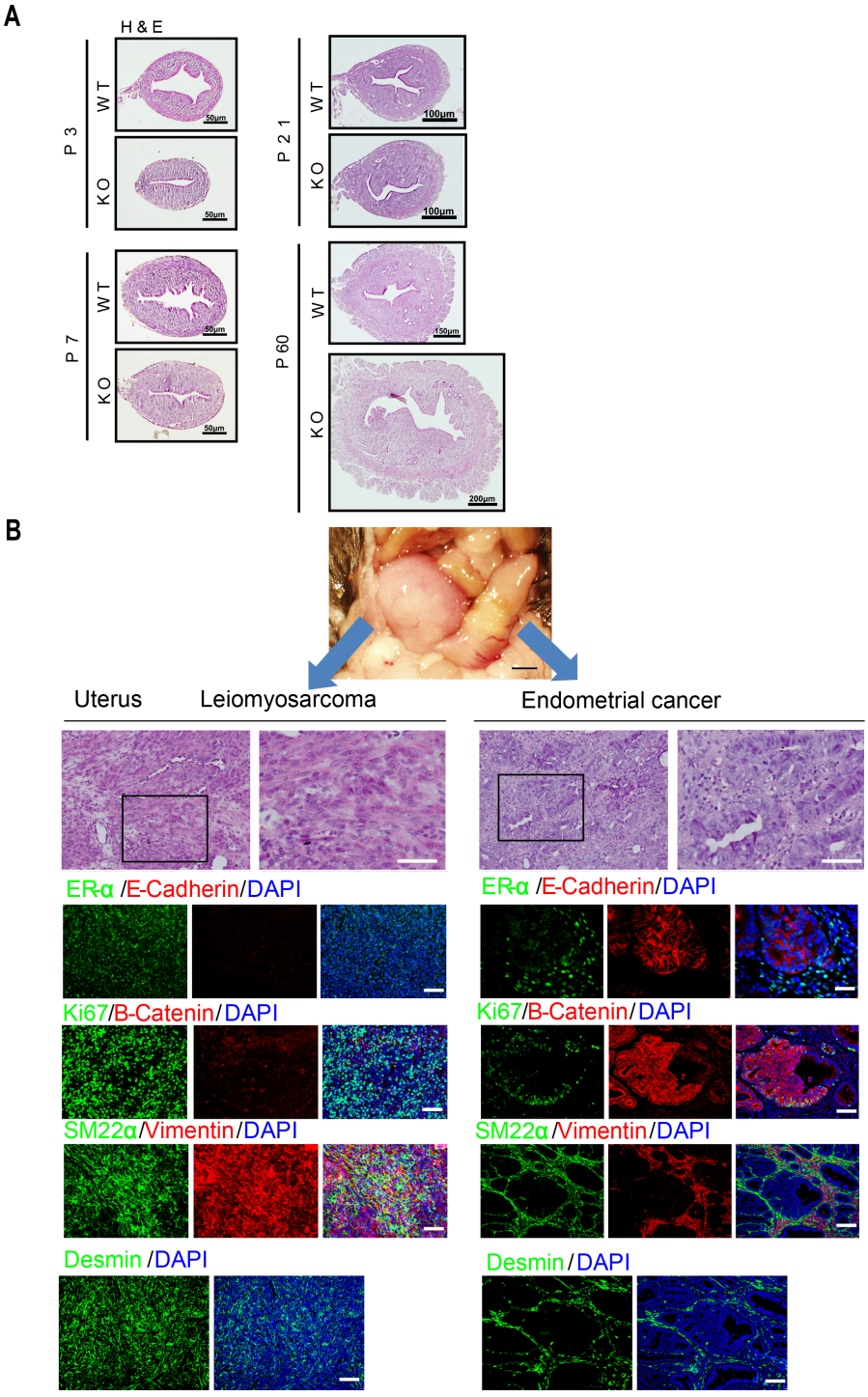

Figure S4. **Deletion of SENP1 in stromal cells significantly induces hyperplasia and tumor formation in aged mice.** Related to Fig.3.

A. Deletion of SENP1 in stromal cells significantly induces hyperplasia. Representative images and H&E staining of isolated uterus from WT and SENP1smKO mice at various ages (postnatal 3, 7, 21 and 50 days. Scale bar: 200 μm. **B.** Deletion of SENP1 in stromal significantly induces tumor formation in aged mice. H&E and immunostaining of uterine tumor sections from SENP1smKO mice at age of 12 months. Sarcoma/endometrial cancer are validated by several markers, including E-cadherin, β-catenin, Vimentin and desmin. Scale bar: 1.0 mm (whole tissue in B); 200 μm (immunostaining in B).

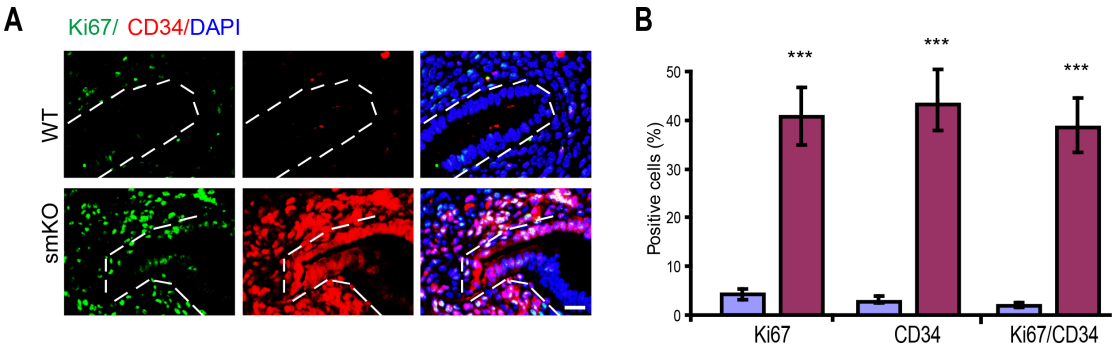

Figure S5. CD34^{+} cells are proliferative. Related to Fig.3.

A. Immunofluorescent staining of CD34 with proliferation marker Ki67 in uteri of WT and SENP1smKO mice at age of 9 and 9 months. **B**. Ki67^{+} and CD34^{+} cells are quantified. All data are presented as means ± SEM, n=5, **, P<0.01 ***, P<0.001 (two-sided student's t-test). Scale bar: 20 μm.

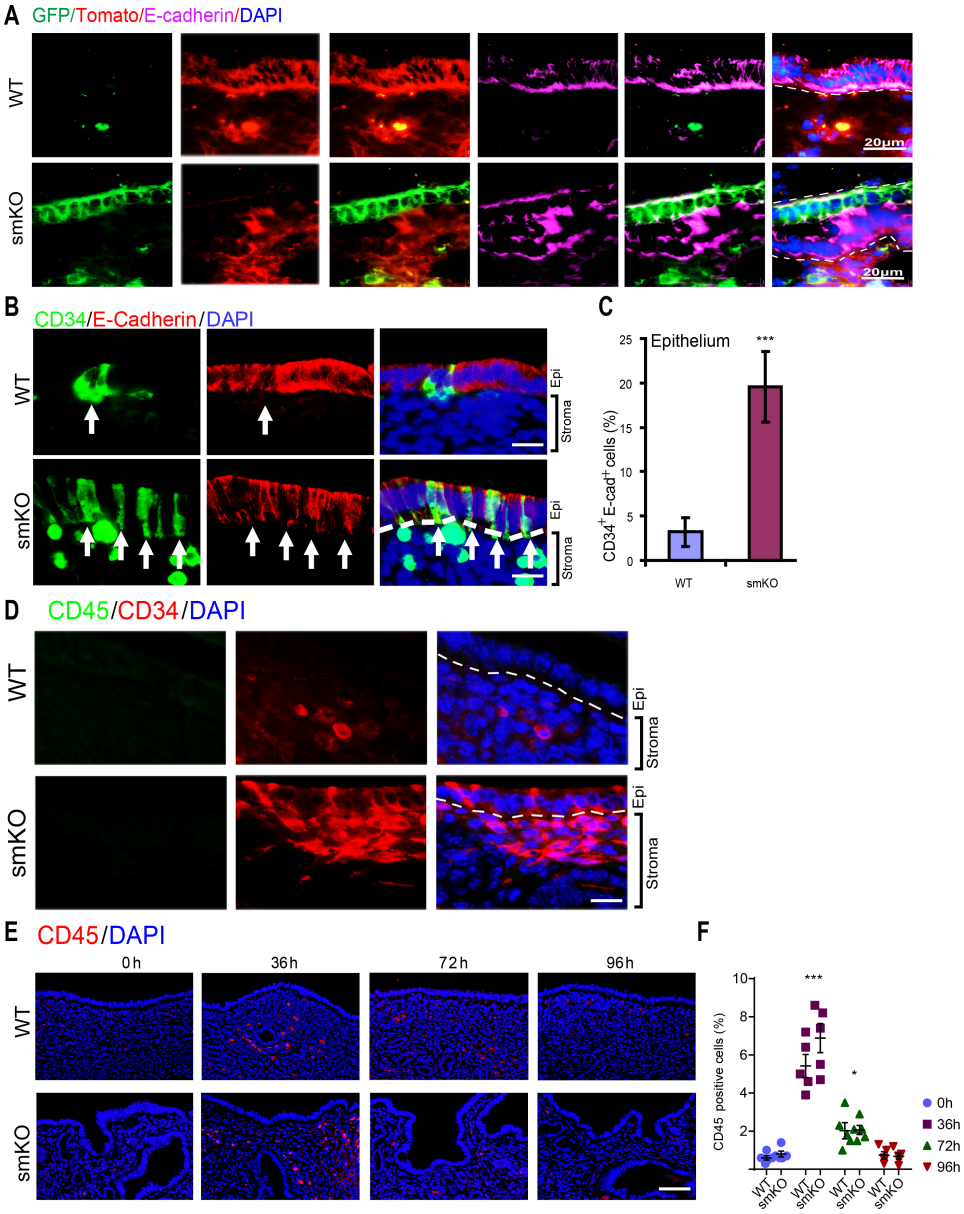

Figure S6. SM22α^{+}CD34^{+} stromal progenitor cells directly contribute to uterine hyperplasia. Related to Fig.4.

A. Immunofluorescent staining with APC-conjugated anti-E-cadherin shown in purple) in uterine sections from mT/mG reporter mice (WT) and SENP1smKO:mT/mG mice at age 2-months old. DAPI was used for counterstaining of cell nuclei. Tomato (mT) indicates SM22α-negative cells whereas GFP^{+} as indicative SM22α-positive cells in stroma and epithelium layer. **B-C.** Co-immunofluorescent staining and quantification of CD34 and epithelial marker E-cadherin in uterine sections of 2-months old WT and SENP1smKO mice. White dash lines show the boundaries between endometrial stroma and epithelium. White arrows show CD34^{+} E-Cadherin^{-} cells in epithelial layer. **D.** Co-immunofluorescent staining of CD34 and leukocyte marker CD45 in uterine sections of 2-months old WT and SENP1smKO mice (n=5). **E-F**. Representative images and quantification of leukocyte marker CD45 in the uteri from a mouse endometrial decidualization model at 0h, 36h, 72 and 96 h post-P4 withdrawal (n=10). All data are presented as means ± SEM, *, P<0.05 ***, P<0.001 (two-sided student's t-test). Scale bar: 20 μm (A,B,D); 100 μm (E).

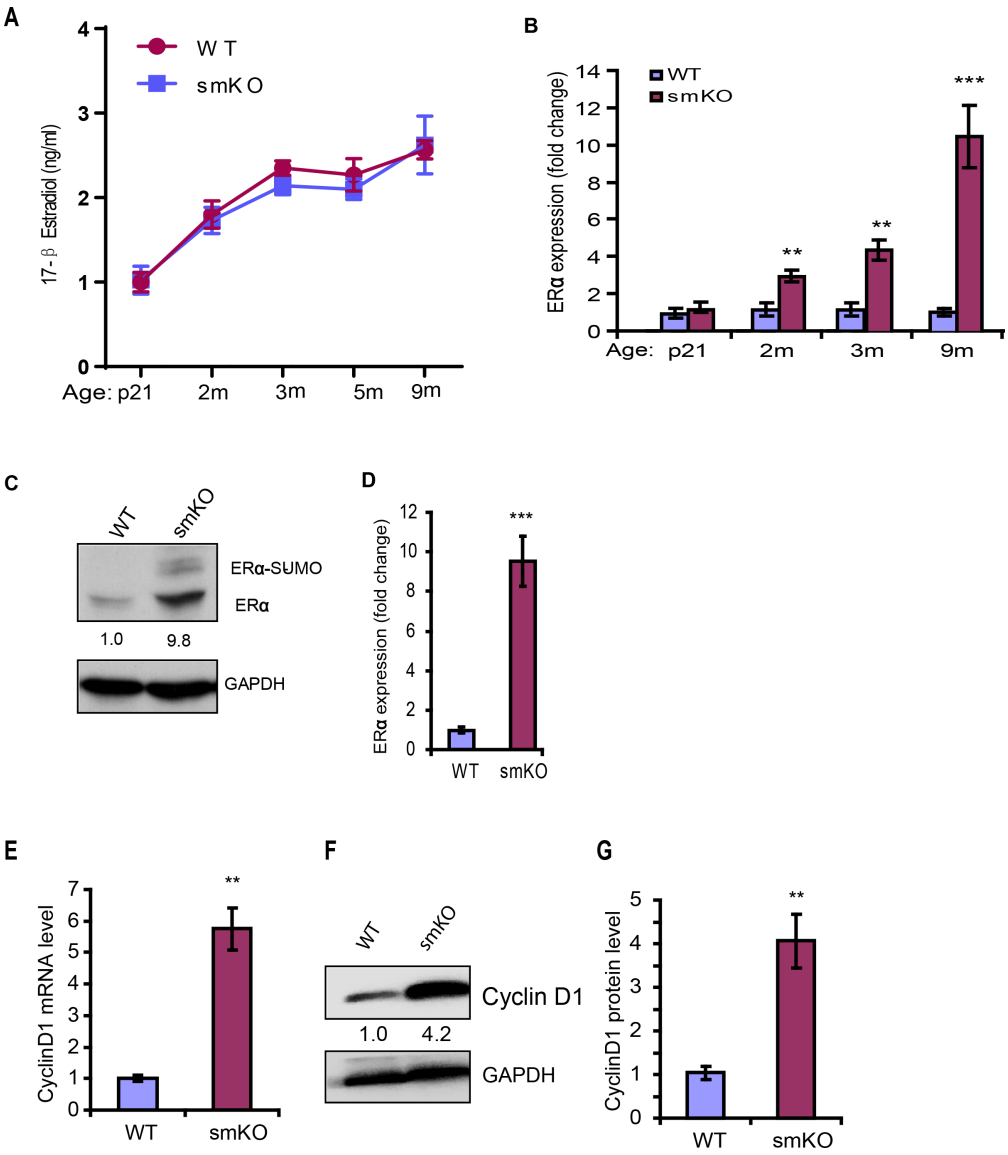

Figure S7. Expression of ERα and Cyclin D1 significantly increased in SENP1smKO mice. Related to Fig.6.

A. 17-β estradiol levels were not different in plasma between WT and SENP1smKO mice. Enzyme-linked immunosorbent assay (ELISA) analysis of 17-β estradiol in serum from WT and smKO mice at various ages.

B. ERα mRNA expression was determined by qRT-PCR in uterus from WT and SENP1smKO mice at various ages.

C-D. Immunohistochemical staining and quantification of ERα in uterine stroma and epithelium from 4-month WT and SENP1smKO mice.

E. Cyclin D1 mRNA expression was determined by qRT-PCR in uterus from 4-month WT and SENP1smKO mice.

F-G. Cyclin D1 protein expression and quantification in uterine from 4-month WT and SENP1smKO mice by Western blotting. GAPDH was used as a loading control.

All data are presented as means ± SEM, n=5, **, P<0.01 ***, P<0.001 (two-sided student's t-test).

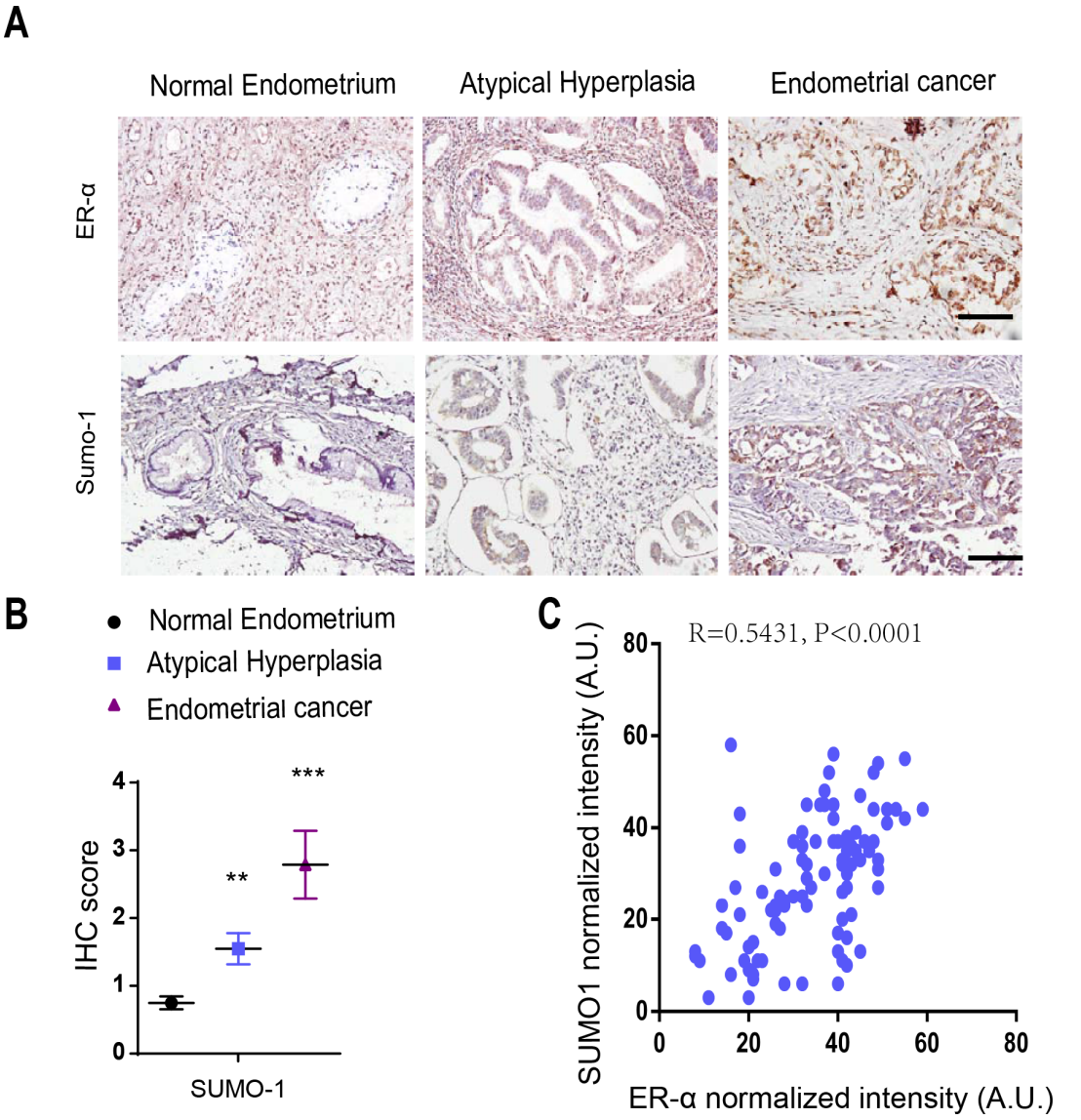

Figure S8. Expression of ERα and SUMO1 significantly increased in human endometrial cancer. Related to Fig.7.

A. Immunohistochemical staining of ERα and SUMO1 in human endometrial cancer samples. Scale bar: 100 μm.

B-C. Relative mean intensity calculated using Image J for cell clusters from 97 endometrial cancer patients. Statistical significance at (R=0.5431, p<0.0001). (two-sided student's t-test).

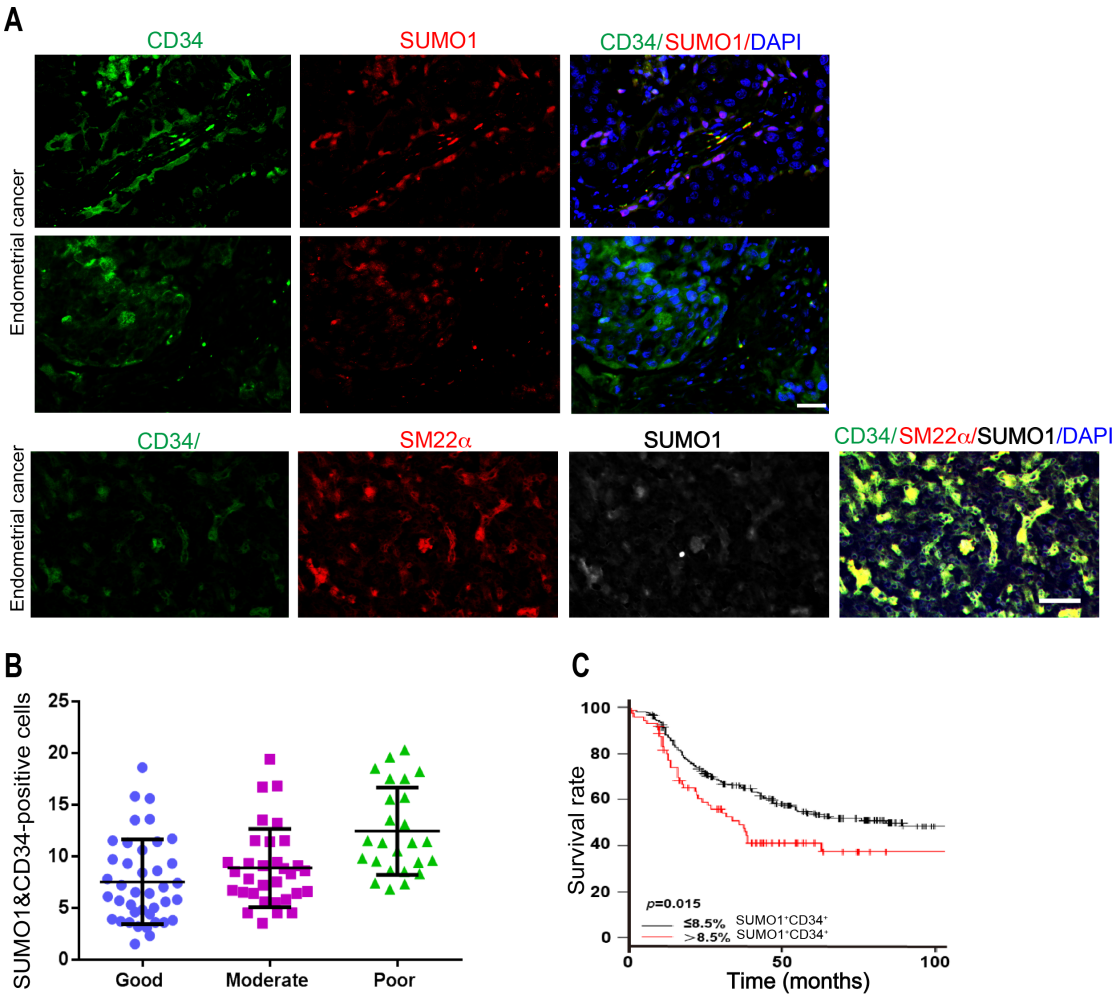

Figure S9. **Expression of CD34 and SUMO1 significantly increased in human endometrial cancer**. Related to Fig.7.

A. Immunofluorescent staining of CD34, SM22αand SUMO1 in human endometrial cancer samples. Scale bar: 50 μm. **B.** Statistical analysis of $CD34^+$ $SUMO1^+$ cells in human endometrial cancer with different histological differentiation (2-sided Student's t test). **C.** Kaplan-Meier curves for OS in human endometrial cancer with low (≤8.5%) or high (> 8.5%) percentage of $CD34^+$ $SUMO1^+$ cells in human endometrial cancer (analyzed with log-rank test)